# Comparison of Kalman Filter and Steepest Descent Method for Assisted History Matching

by

Faranadia Binti Ab Aziz

13800

Dissertation submitted in partial fulfillment of

the requirements for the

Bachelor of Engineering (Hons.)

(Petroleum)

FYP II May 2014

Universiti Teknologi PETRONAS
Bandar Seri Iskandar
31750 Tronoh
Perak Darul Ridzuan

# CERTIFICATION OF APPROVAL

## Comparison of Kalman Filter and Steepest Descent Method for Assisted History Matching

by

Faranadia Binti Ab Aziz

13800

A project dissertation submitted to the

Petroleum Engineering Programme

Universiti Teknologi PETRONAS

in partial fulfillment of the requirements for the

BACHELOR OF ENGINEERING (Hons)

(PETROLEUM)

Approved by,

_____

(Name of Main Supervisor)

UNIVERSITI TEKNOLOGI PETRONAS

TRONOH, PERAK

May 2014

# CERTIFICATION OF ORIGINALITY

This is to certify that I am responsible for the work submitted in this project, that the original work is my own except as specified in the references and acknowledgements, and that the original work contained herein have not been undertaken or done by unspecified sources or persons.

_____

FARANADIA BINTI AB AZIZ

# ACKNOWLEDGMENT

First and foremost, I would like to dedicate a special thanks to my supervisor, Mr. Berihun Mamo Negash, for his guidance in completing this Final Year Project with his full effort and willingness to share his knowledge with me.

I would like to express my deepest gratitude and appreciation to all parties that had been involved, directly or indirectly, in making this project a success which is very meaningful to me. Throughout this whole two semesters, I have learned various new knowledge and gain valuable experience that will be useful for my career in the future.

## Table of Contents

## List of Figures

**List of Tables**

# ABSTRACT

Every new generation of petroleum industry always search for new reliable method to approximate reservoir parameters in high resolution for long periods and large number of grid blocks for reservoir management purposes. History matching is a system that reduces the difference between the model performance and its historical behavior. There are many discoveries of optimization methods that can be applied for history matching purposes, but not all methods are suitable and reliable enough.

This report studies the process of history matching, demonstrates some of the steps required and then review and compares the application of one method over another method for assisted history matching purpose. Assisted history matching is a technique that integrates forward model, formulation of an objective function and optimization. Among all of the optimization methods of history matching, Kalman filter and steepest descent methods are chosen. Steepest descent is one of the gradient based methods while Kalman filter is a non-gradient based method. Both of these methods are investigated and the results are compared.

Two different sets of reservoir parameters of synthetic model are used to obtain both historical and simulated model and production data. Forward model is constructed and an objective function also is obtained in order to observe the discrepancy between the calculated and historical data. Hence, this report compares Kalman filter and steepest descent methods in order to investigate the more reliable methods that can provide better result in terms of their accuracy, CPU time and reliability for assisted history matching.

# CHAPTER 1

# INTRODUCTION

## 1.1 Background of Study

Prediction or estimation of data is a very difficult process because it involves things that will happen in the future. [1] mentioned that poor information on distributed system properties will cause the uncertainties increase to a level where quantification of uncertainties may become the main problem in implementation tasks. Therefore history matching can helps to decrease the uncertainties and improve the estimation system. Indeed, as stated by [2], history matching in reservoir application is a difficult inverse problem in oil and gas industry. History matching is described by means of the process of altering a reservoir model until it thoroughly similar to the performance of the historical reservoir. Based on [3], the main purpose of implementing the history matching is to minimize the discrepancy between the behavior of the simulated model and the historical reservoir. Basically, history matching is classified into manual history matching, assisted history matching and automatic history matching. [4] mentioned that manual history matching is a try and error technique where it is difficult to be implemented since the reservoir behavior is complicated and the approximated data may be greatly interacting. Hence, the petroleum industry creates an assisted history matching and automatic history matching to overcome the problem encountered in manual system. It is stated in [5] that the assisted history matching reduces a cost function which calculates the dissimilarity between observed and simulated production rates. In the meanwhile, automatic history matching as defined by [4] as a technique where estimates parameter value will be used to minimize a performance index thus this new technique becomes a mathematical minimization problem.

The history matching system can be viewed as three stage procedures where the first step is constructing a mathematical model which also known as forward model. According to [6], this forward model involve two elements for the prediction of the unknown parameters, which are a reservoir flow simulator such as ECLIPSE to signify the fluid flow over the porous media, and the other elements are rock physics model which are PEM and FWSM. Second step is obtaining the objective function where it is described as the difference between the reservoir observation data for example the production previous data. [6] also stated that there are three types of formulation to obtain the objective function which are least-square formulation, weighted least-square formulation and generalized least-square formulation. Thus, for this project, weighted least-square formulation will be used in order to find the discrepancy between the historical and calculated data. Third step is the optimization process. Two methods will be analyzed, which are the Kalman filter and steepest descent methods.

According to [7], the Kalman filter has been around for about 50 years where it was developed by Rudolph E. Kalman in 1960 who published his well-known paper defining a recursive solution to the discrete-data linear filtering problem. Regarding [8], Kalman filter is a mathematical power tool that become a progressively significant role in computer graphics. It is the best potential and effective estimator even for a large problems case. The Kalman filter is basically a set of mathematical equations that apply a predictor-corrector type of optimal estimator where it reduces the approximated error covariance when some assumed conditions are encountered. Since Kalman filter is introduced, it has been the topic of broad research and implementation, predominantly in reservoir estimation area, autonomous and assisted navigation. It is possibly due to relative simplicity of the filter and developments in digital computing that cause the use of the filter feasible. The first attempt to modify this filter to nonlinear problems was done by applying the Extended Kalman Filter (EKF), where it linearized the nonlinear model using the Jacobian. However it is not acceptable for big scale problems or too nonlinear problem. Hence to handle large nonlinear oceanic models, the Ensemble Kalman Filter (EnKF) was presented by Evensen in 1994, and has had bright outcomes in many areas.

The other method is one of a gradient based method, steepest descent or also called as gradient descent method. This method first developed by Riemann in 1892. It is about finding the closest local minimum of a function which assumes that the gradient of the function can be determined. Although both methods have been implemented successfully in some field, but they still have their own disadvantages. For gradient based method referring to [9], the problems is in parameter prediction and monitoring network design while for the non-gradient based in [10], it requires a huge number of design cycles. Hence, this report described the comparison between both Kalman filter and steepest descent methods for assisted history matching and will conclude which method is more feasible to be implemented.

## 1.2 Problem Statement

Reservoir history matching is a challenging inverse problem arising in the oil industry because it involves with large number of unknown and uncertainties during the estimation and forecasting process. In response to this problem, steepest descent, a gradient based and Kalman filter, a non-gradient based optimization techniques are progressively implemented by the petroleum industry for computer-aided history matching. Steepest descent is fast in each iteration but it needs a lot of iterations to reach the minimum or the definite point. On the other hand, Kalman filter is a robust and optimal linear quadratic estimator however it is computationally complex especially for large numbers of sensor channels. Therefore, Kalman filter and steepest descent methods are compared in order to choose either one of the methods can provide more accurate estimation in reservoir application with great CPU time saving benefits for assisted history matching purpose.

## 1.3 Objectives and Scope of Study

The main objective of this report is:

- To analyze and compare two optimization methods, Kalman filter and steepest descent on which method is best to be implemented and provide a more accurate result for assisted history matching.

The scope of this project is limited to synthetic model where synthetic model is used instead of the actual reservoir model. The reason is because the number of parameters and the value of the actual model are too large and it has a number of data issues regarding the data outlier, missing values, and data drift.

Two methods are analyzed which are one from gradient based method called steepest descent while the other one is non-gradient based method called Kalman filter. Even though there are many other gradient and non-gradient methods, but through the preliminary study, Kalman filter and steepest descent have been proved as two most commonly implemented. Hence, both of these methods are analyzed in order to contribute to the industry by investigating and suggesting the best method to be applied for history matching based on the knowledge and experiences as an undergraduate student.

## 1.4 Relevancy

This project is relevant since history matching is a very important and difficult technique in petroleum industry. This project will contribute in suggesting the industry to practice the best minimization algorithm for assisted history matching. The reason of analyzing both of these methods to the assisted history matching is to compare between two most implemented methods. The advantage and disadvantages of each methods are identified and it has been decided which one of them is easier to be implemented, more reliable and beneficial to the industry.

# CHAPTER 2

# STATISTIC FUNDAMENTALS

For gaining the understanding of Kalman filter method, it is very essential to understand the statistic fundamentals. [7] demonstrated a great overview of the basic statistics so that the reader can easily understand the filter theory. All of these terms will be used in explaining the Kalman filter method later.

## 2.1 Random variables

Random variables are which the value is subject to variation due to chance. A real random variable is a real finite-valued function X (·) described on sample space, Ω if the inequality for every real number is:

$$X(\omega) \leq x \tag{1}$$

ω is the defined probability.

## 2.2 Probability density function

Probability density function (PDF) is the density of probability around given value chances for random variable to take on specified value. The PDF $fX\ (x)$ must satisfy equation given:

$$fX(x) \geq 0 \tag{2}$$

$$\int_{-\infty}^{\infty} fX(x)dx = 1 \tag{3}$$

## 2.3 Variance and covariance

**Variance**

The variance of a random variable is stated in Equation (4) below:

$$\text{V AR(X)} = [\text{E}(X\ -\ E[X])^2] = \text{E}\ [X^2] - \text{E}[X]^2 \tag{4}$$

In a qualitative sense, the variance of Xi is a measurement of the dispersion of X around its mean. Zero variance means all values are identical. Other assets of the random variable X is the standard deviation ($\sigma$), or the square root of the variance.

**Covariance**

The covariance determined below in Equation (5) for two random variables of X and Y.

$$\text{COV}\,[X, Y] = \text{E}\,[(X - \text{E}[X])\,(Y - \text{E}[Y])] \tag{5}$$

The joint probability function can be specified as f(X, Y). If X and Y are independent, f(X, Y) = f(X) f(Y) and therefore COV [X, Y] = 0. Qualitatively the covariance defines the reliance between both random variables X and Y.

## 2.4 Probability distribution

Random variables have a definite distribution given by their PDF. There are many distributions for random variables which the most common is the normal or Gaussian distribution. The Gaussian distribution PDF is specified by Equation (6):

$$fX(x) = \frac{1}{\sqrt{2\sigma^2}}\left[-\frac{1}{2\sigma^2}(x - E[X])^2\right] \tag{6}$$

The normal distribution consists of distribution function and probability density function (PDF) as demonstrated in Figure 1. Below the CDF and PDF are plotted for dissimilar standard deviations $\sigma$ given a Gaussian distribution. X~N (E[X], $\sigma^2$) is a simple way to express that random variable X is normal distributed with an expected value of E[X] and standard deviation $\sigma$. When X is a vector of Gaussian distributed random variables with covariance matrix Q and mean E[X], then this can be indicated X~N(E[X],Q). The diagonal component of Q symbolizes the variance for every random variable in X and the off-diagonal components denote the covariance between the variables.

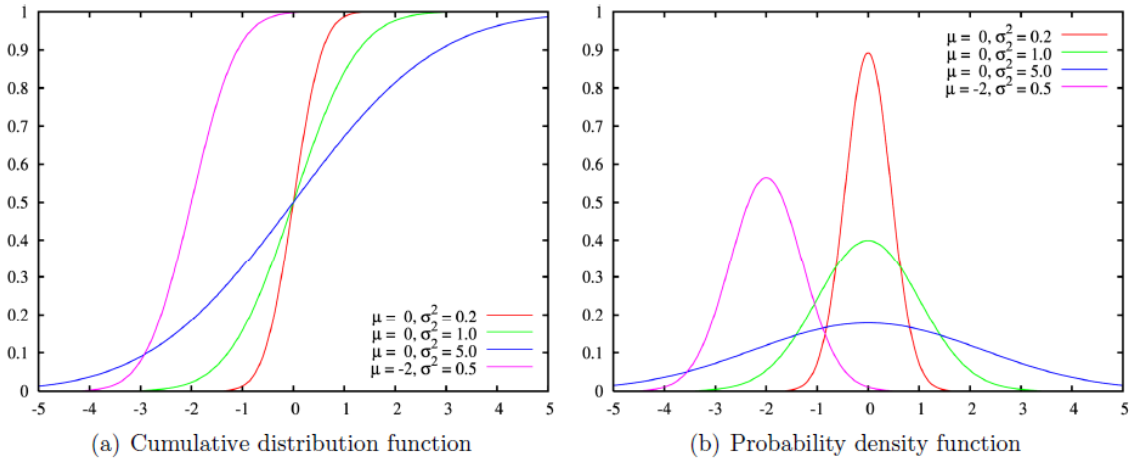


*Figure 1: CDF and PDF for Gaussian distribution*

(Source: John Petter Jensen, 2007) [7]

# CHAPTER 3

# LITERATURE REVIEW

## 3.1 Background of History Matching

History matching as stated by Dean S. Oliver and Yan Chen [11] is an inverse problem where the experimental reservoir characteristic is apply to predict the reservoir model variables that create the characteristic. Inverse problem is described as determining the unknown model parameters that lead to the solution when the result is already known. For both forward and inverse problems, the physical structure is categorized by a set of model parameters, either a function or a scalar. In the case of steady state single-phase flow problem, the model parameters can be selected as the inverse permeability ($m(x) = 1/k(x)$), fluid viscosity, length L and cross sectional area A. For example in this book for the steady-state problem, it is defining the permeability from pressure data measured at points in the interval [0, L]. Pressure calculations are subject to noise, hence measured pressure data will not be accurate. Therefore, it is important to recognize the best estimate of uncertainty, either in the parameters or in function of the parameters.

In addition, Heimhuber, R. [1] mentioned that limited information on distributed system properties such as permeability and porosity can cause the quantification of uncertainties become the main problem in application tasks. Uncertainty generally begins when models are being used without comprehensive knowledge of all essential parameters. Calibrating models for underground reservoirs on historical production data which called history matching can diminish uncertainties and thus improve the forecasting power. Nevertheless, history matching complex models is a very difficult problem. Therefore an advanced framework for model calibration and history matching using polynomial chaos expansion (PCE) is proposed. The structure comprises two major stages. In the first stage, the original full complex model is projected onto a response surface via PCE, which is an extreme and proficient model reduction. Second stage

involves Bayesian updating in order to match the minimized model to existing measurements of other real-time observations of system characteristics or state variables. Considering the reduced model is enormously more effective than the original model, it is feasible to accurately updating parameters much beyond brute-force optimization.

Regarding to Van Doren, J., et al [12], they claimed that the objectives of history matching improve the estimated capacity of a reservoir simulation model by modifying the model parameters until the gap between simulated model and the historical model is minimized. The computational cost of this method is not depending on the number of variable but on the number of objective functions because this method provides the gradient of a specified objective function respecting to all applied variables by running several simulation. This technique is most suitable for structural updating of huge scale reservoir models using production data or time-lapse seismic. However Dadashpour, M. [15] claimed that the adjoint method needs access ability to the simulator code and derivative information which are an accurate estimation that in some real study it is not likely to have access to them. Moreover, adjoint codes are not easy to compose, and the reliability can be a problem.

While on the other side, M. R. Abdel-Rahman, et al [13] demonstrated a new approaches to validate history matching results because they mentioned that history matching is the highest challenging process and time intensive for reservoir simulation domain. He defines new workflow to incorporate all historical data from field observation and demonstrate change of fluid distribution over fluid production history such as surveillance of water coning and oil water contact encroachment. 3D modeling platform, Petrel is used to assimilate all of these data in automated system to construct conceptual 3D fluid distribution models at chosen time augmentations that signify the past field production. There are two major steps in the workflow where the first step is using geo-statistical technique to interpolate available fluid change surveillance at well level to build fluid contact surfaces at selected time increments while the second step is using Petrel to form corresponding 3D conceptual fluid distribution model to define fluid profile at a time.

There are three types of history matching which are manual history matching, automatic history matching and assisted history matching. Based on R. Rwechungura, et al [6], manual history matching is defined as a manual trial and error system in updating the reservoir parameters. Reservoir engineers evaluate the discrepancy between observed and simulated value, then manually alter one or several parameters at one time expecting to improve the match. In some system, reservoir parameters are manually updated normally in two steps which are saturation and pressure match. Manual history matching is concluded as not reliable in long terms with a lot of uncertainties since reservoir generally is very heterogeneous. There are thousands number of grid blocks and even more in a normal simulation model and it is hugely depends on engineer knowledge, experience and budget. On the other hand, automatic history matching is said as a method of employing the computer to alter the parameters which is an inversion problem. This project will focus on the assisted history matching. The definition of assisted history matching is described by C. Yang, et al [14] as a semi-automatic method where the reservoir engineer apply his experience and engineering understanding assisted by computer program for the history matching purpose. It is a creation of initial model and initial estimation of reservoir parameters, and then undergoes an organized reduction process of objective function which it symbolizes the incompatibility between calculated and observation response by concerning the related parameters. This technique reduces the time spent by the reservoir engineer to create models comprising different parameters values and assessing the results of the simulation.

### 3.2 Assisted History Matching

In general, there are two categories of assisted history matching technique. First technique is known as direct assisted history matching and second technique is known as indirect assisted history matching. For direct assisted history matching, each step in the optimization procedure relates to one reservoir simulation. The objective function of all solution of each step is directly assessed by reservoir simulation. Figure 2 show the example of direct AHM workflow where it shows that this technique desires to run reservoir simulations simultaneously until the smallest objective function is attained.

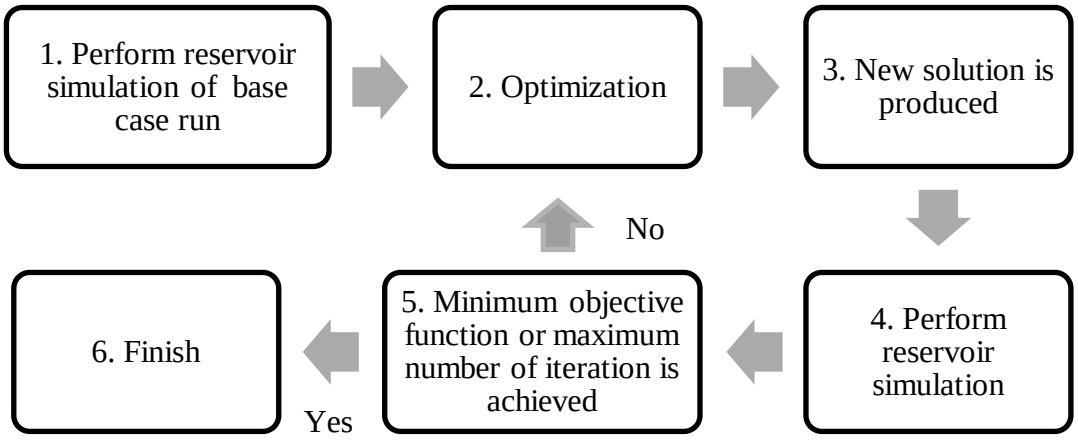


*Figure 2: Workflow of direct assisted history matching*

### 3.3 Implementation of History Matching

According to Rwechungura, R.W., et al [7], he found that Kruger is the first to develop the history matching in 1961 where he computed the reservoir's areal permeability distribution. In 1965, Jacquard and Jain expanded a technique to automatic history matching. Watson et al. in 1979 analyzed history matching in two-phase flow while in 2003, Li et al. investigated an adjoint method, three-dimensional, three-phase reservoir flow production data in history matching in order to reduce discrepancy in wellbore pressure flow, generating water oil ratio (WOR) and gas oil ratio (GOR). A genetic algorithm is applied to complex synthetic teen-layers reservoir model in history matching by Romero and Carter in 2001. Next, Rotondi et al. in 2006 implemented the neighborhood algorithm to seven wells and six years production history. In 2013, R. H. Lind et al. have tested to fine tune individual well matches by using computer assisted history matching and the result of the well matches have been prominent. While recently in 2014, Fabio Ravanelli and Ibrahim Hoteit [15] demonstrated the application of time-lapse crosswell data as the alternate source of time-lapse data to improve history matching. The development of history matching is still continuing until recent years in order to make improvement and ease the implementation of this technique.

Van Doren, J., et al [12] demonstrated a very good implementation of adjoint-based history matching of structural models using production and time-lapse seismic data. He

believed that updating of structural parameters can increase the history match quality which needs to be implemented in static model, not only in dynamic flow model. He was demonstrating three experiments by applying a gradient based history matching method which is adjoint-method to effectively calculate the derivatives of data discrepancy with regard to porosities of the grid block and transform the corresponding volume changes to structural updates which is the layer thicknesses in the static model.

The workflow of the gradient-based history matching of structural parameters is presented schematically in Figure 3 below.

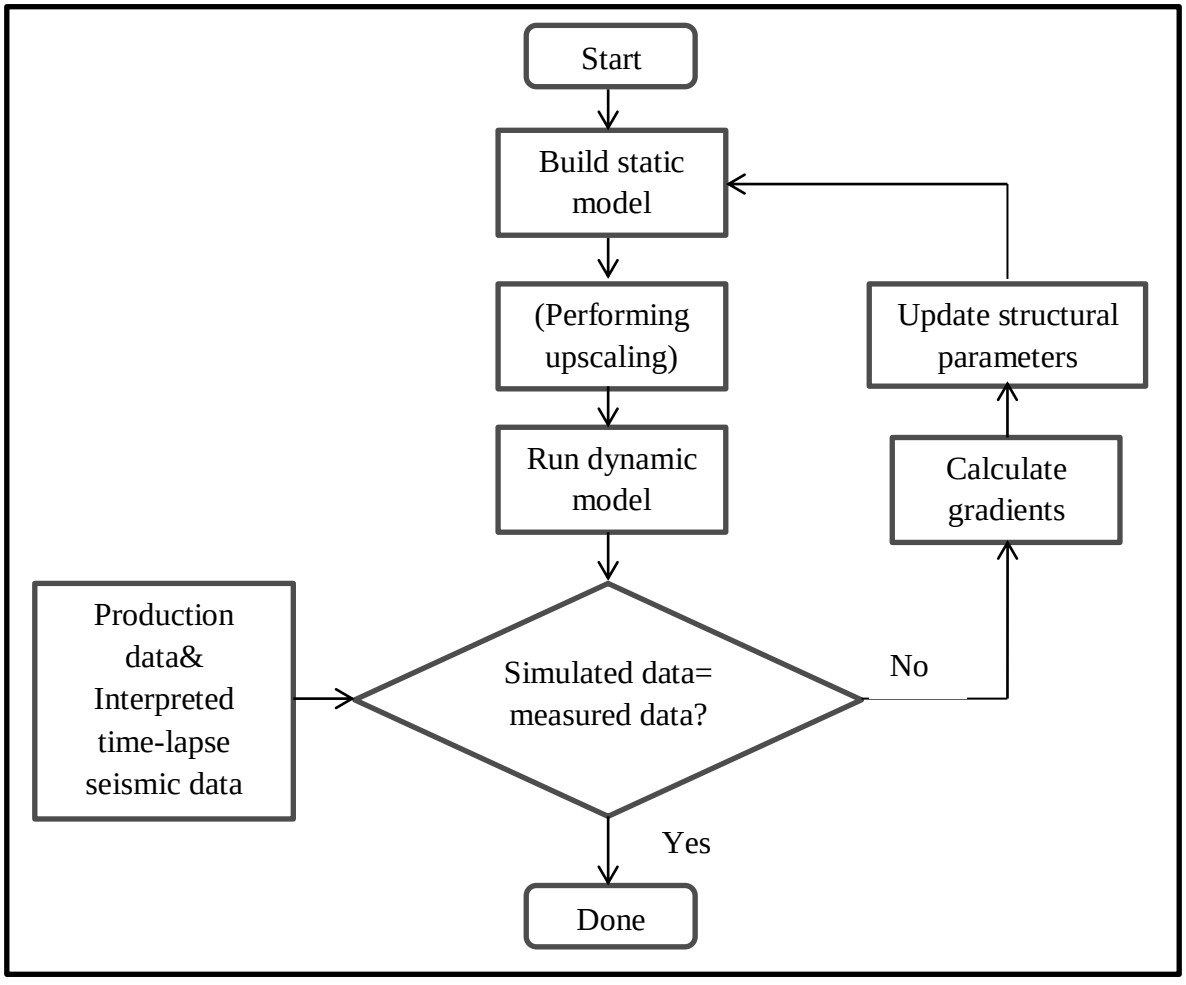


*Figure 3: Workflow for gradient-based history matching of structural parameters in static model.*

(Source: Van Doren, J., et al, 2013 [12])

**Experiment: Assimilation of Time-Lapse Data**

The truth model illustrated a modest three layers, three dimensional reservoir with impermeable shale layer in between top and bottom permeable zones. At the beginning of the production, the injectors were injecting at a constant flow rate of $300m^3$/day while the producers have a bottom hole pressure of 39 MPa at the top perforations. The truth model is built to generate synthetic production data for 12 years. The measurements such as water rate and oil rate per well are taken every month. These experiments were conducted after 8 years of production. Interpretation of time-lapse seismic data is signified as changes of saturation per grid block. Figure 5 below illustrates the oil saturation after 8 years producing in the bottom layer of truth model.

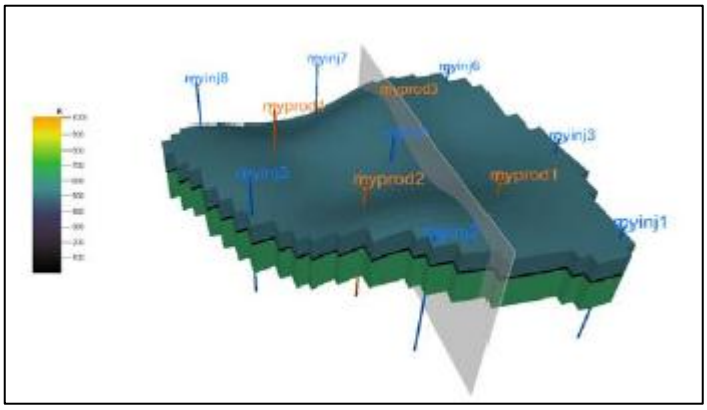


*Figure 4: Truth model permeabilities. Seven injectors are located around the field and one at the center. Four producers are placed at the center of the field. The transparent plane shows the cross section.*

(Source: Van Doren, J., et al, 2013 [12])

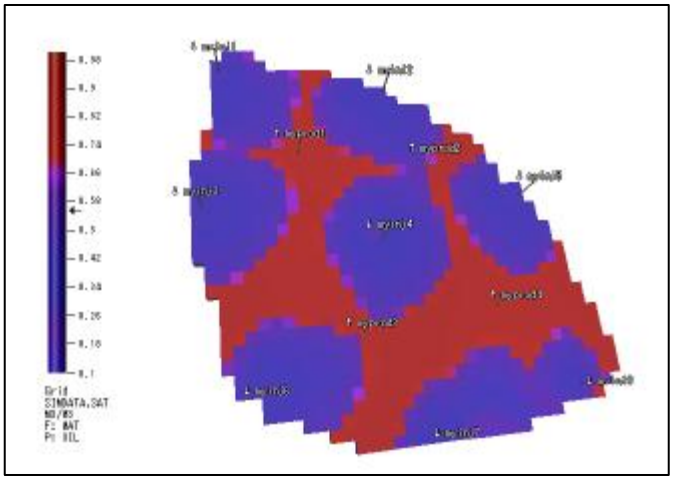

*Figure 5: Oil saturation in truth model's bottom layer after 8 years producing.*

(Source: Van Doren, J., et al, 2013 [12])

Demonstrated here in Figure 6 is the third experiment which comprises assimilation of time-lapse seismic data instead of production data. This experiment starts from unsatisfactory prior, and then includes the assimilation of time-lapse seismic data as an alternative of production data. The step length selected was 3.5 and after 30 iterations, the objective function value is decreased by factor of ten.

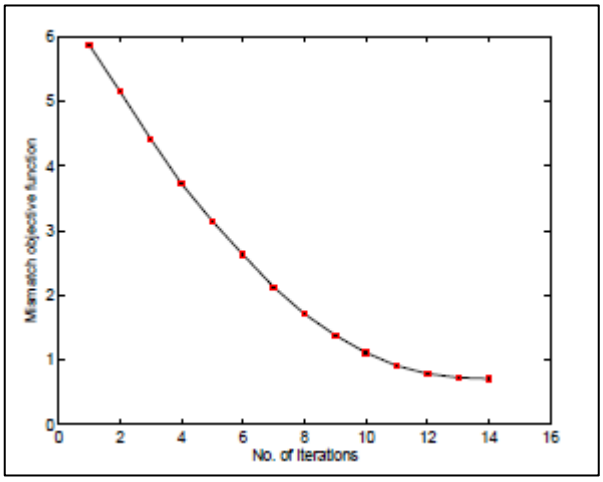


*Figure 6: Mismatch objective function*

(Source: Van Doren, J., et al, 2013 [12])

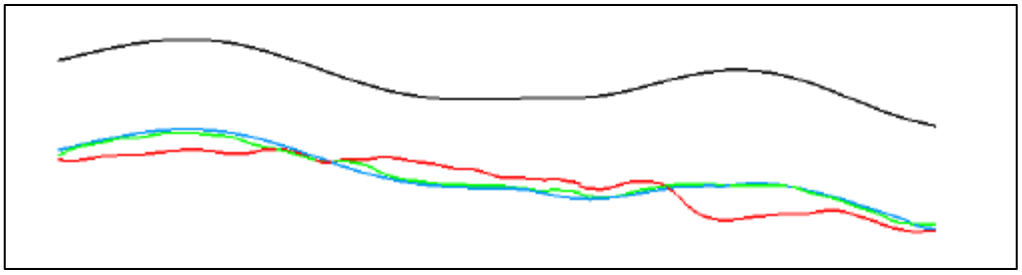

*Figure 7: Cross section through the bottom layer of the reservoir. Blue color symbolizes the truth, red symbolizes prior, and green symbolizes the updated model.*

(Source: Van Doren, J., et al, 2013 [12])

Figure 8 below shows the prior and updated depths of the bottom horizon and Figure 9 shows the corresponding residual maps. Compared to the previous experiment which performs the assimilation of production data, history matching of the bottom horizon which involved assimilation of time-lapse seismic data comes out in a satisfactory mismatch objective function value and better match between the truth model and updated.

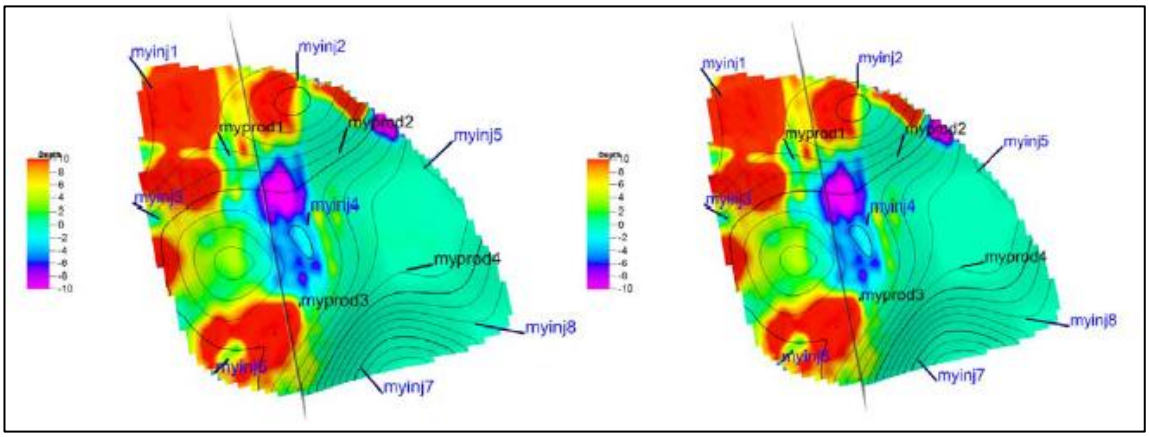


*Figure 8: Prior (left) and updated (right) residual maps of previous experiment. The colors symbolize the residuals in m. Contour lines specify the true bottom depth.*

(Source: Van Doren, J., et al, 2013 [12])

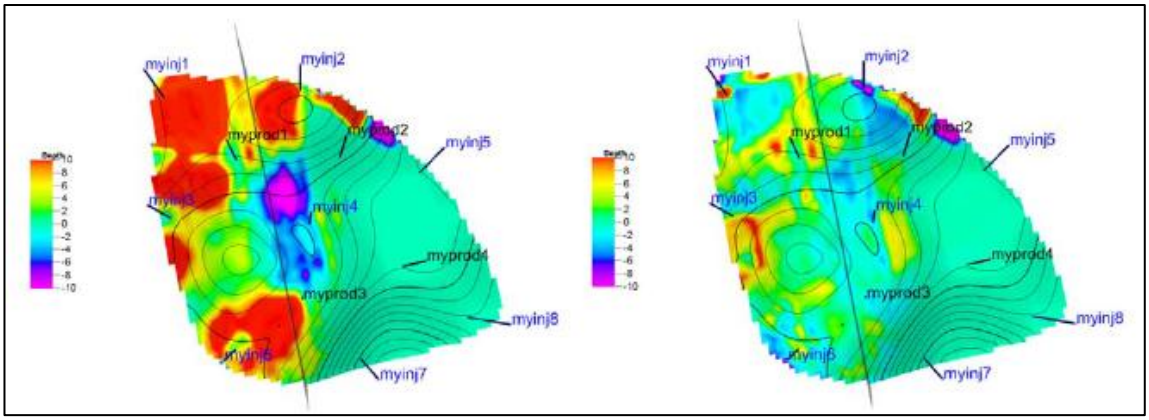


*Figure 9: Prior (left) and updated (right) residual maps. The colors symbolize the residuals in m. Contour lines specify the true bottom depth.*

(Source: Van Doren, J., et al, 2013 [12])

Figure 10 below represents the oil flow rates of the four production wells along 15 years of production for Experiment 3. The production begins in 2004 and a time-lapse seismic survey was performed and the interpreted outcomes are assimilated. The curves symbolize estimation of future oil production. The results of performing assimilation of time-lapse seismic data instead of production data are very good where the simulated oil flow rates of updated model are match perfectly with the measured rates. In addition, the estimated flow rates are much closer to the truth compared to those simulated using the prior model.

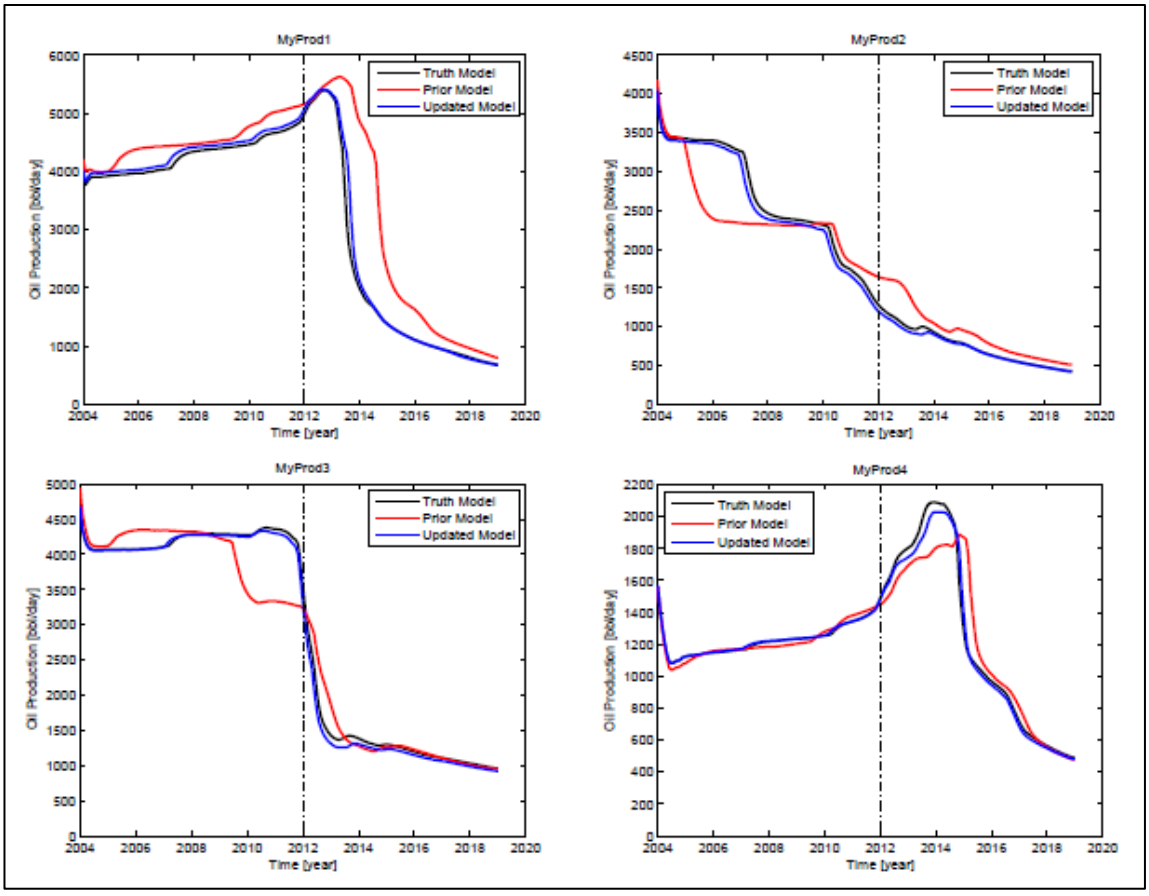


*Figure 10: Oil flow rate of each of the four production wells for the Experiment 3. Red curves denote the prior model simulation rates, blue curves denote the updated model rates and black curves denote the truth model rates. The vertical dashes line illustrates the moment of performing history matching.*

(Source: Van Doren, J., et al, 2013 [12])

## 3.4 Procedures of History Matching

There are three procedures to implement history matching referred to Trondheim [15], which are constructing a forward model, obtaining the objective function and then going through the optimization process. Figure 11 below shows the flow of the inversion process. This system traditionally begins from an initial estimate of model parameters and then the procedure is repeated until the greatest fit is achieved between the observed and calculated data. For this project, permeability is chosen as the optimization variable

based on sensitivity analysis while production data as the output or observations variables.

The most commonly used algorithm for an inversion procedure is:

1. Construct initial guess for the model parameters,

2. Calculate the response of the system from the forward model,

3. Calculate the objective function,

4. Update the parameters by reducing the objective function by applying minimization systems ($D_{obs}$ is the initial guess, and then by using the forward model constructed, $d_{cal}$ can be obtained),

5. If the objective function value is not small enough, repeat step two.

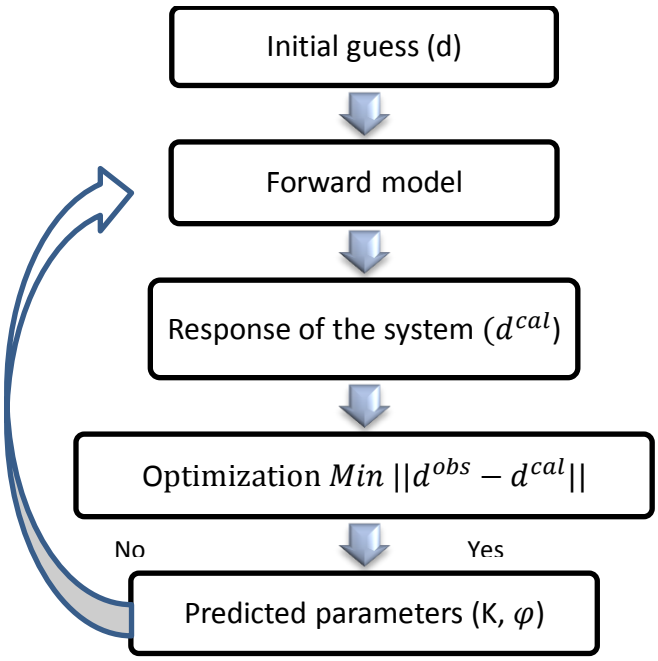


*Figure 11 Algorithm for inversion process*

## 3.5 Optimization Algorithms for History Matching

There are gradient and non-gradient methods for optimization in history matching based on Rwechungura, R.W., et al [6]. The gradient methods include Steepest Descent, Gauss-Newton, and Conjugate Gradient while non-gradient methods include Kalman Filter, General Pattern Search and Nelder-Mead.

### 3.5.1 Gradient Methods

**Steepest Descent**: The steepest descent or also called as gradient descent is a first-order optimization algorithm. To find a local minimum of a function using steepest descent, negative gradient vector must be used at every point as the search direction for each iteration. The gradient vector must be orthogonal to the plane tangent to the isosurfaces of the function. Steepest descent can solve a linear equations system and reproduced as a quadratic minimization problem.

**Gauss-Newton**: The Gauss–Newton algorithm is a technique used to solve non-linear least squares complications. It is a modification of Newton's system for searching a minimum of a function, but it has the benefit which challenging to calculate the second derivatives are not necessary. However for some functions, Steepest Descent is said to be much more dependable.

**Conjugate Gradient**: The conjugate gradient method is an algorithm for the linear equations systems which positive-definite and has symmetric matrix. It is regularly implemented as an iterative process, suitable for too large sparse systems that are difficult to be handled using a direct implementation such as the Cholesky decomposition.

### 3.5.2 Non-Gradient Methods

**Kalman Filter**: The Kalman filter, also acknowledged as linear quadratic estimation (LQE), is an algorithm that practices measurements observed over time, comprising noise and inaccuracies, and obtains estimates of unknown variables that are more precise than other methods in terms of a single

measurement alone. It works recursively on streams of noisy input data to build a statistically optimal approximation of the original system state.

**General Pattern Search**: Pattern search (PS) can be applied on discontinuous or differentiable functions. It differed one theoretical parameter by steps of the similar scale, but when there are no any changes in any parameter to improve the fit to the experimental data, the step size need to be halved and repeated the procedure until the steps are considered small enough.

**Nelder-Mead**: The Nelder–Mead is a regularly used nonlinear optimization method, a method for reducing an objective function in many dimensional spaces and a well-defined numerical process for unknown derivatives problems.

One of gradient based method which is steepest descent and one of non-gradient based method which is Kalman filter will be further explained.

### 3.6 Steepest Descent for History Matching

Analyzing the implementation of steepest descent method for history matching purpose, P. H. Yang and A.T. Watson [4] demonstrate the comparison between two variable-metric minimization methods which are the Broyden Fletcher Goldfarb Shanno (BFGS) and self-scaling variable-metric (SSVM) methods, and two previous minimization methods which are steepest descent and conjugate-gradient methods for optimal-control theory implementation, tested with hypothetical two-phase reservoir history-matching problems. He described history matching as the technique of estimating the properties by altering parameters using numerical simulator so that simulated pressure match with the production of field data. In his paper, he estimated rock and fluid properties such as porosity, permeability and relative permeability. In automatic history matching, the estimates are normally selected as parameters that reduce a performance index.

BFGS method was selected because it is commonly considered as the most optimal choice between all variable-metric methods and has numerous appealing properties. On the other side, selection of SSVM methods was based on quadratic performance index. Even though SSVM methods are usually not as effective as BPGS method, it can be

very efficient in some circumstances for instance when the objective function comprises high variables powers or when there are large numbers of variables.

**Case Studies**

Four cases were tested based on hypothetical water floods of one-dimensional reservoir model were demonstrated. The study was using ten grid blocks of reservoir model with one injection well and a producing well. Complete model interpretation and test cases is shown in Table 1.

| Fluid and Reservoir Properties | |
|---|---|
| $k$, darcy* | 0.08 |
| $\phi$** | 0.3 |
| initial $p$, atm | 50 |
| $\mu_o$, cp | 5 |
| $\mu_w$, cp | 1 |
| initial $S_w$ | $S_{wi}$ |
| $c_o$, atm$^{-1}$ | $1 \times 10^{-4}$ |
| $c_w$, atm$^{-1}$ | $1 \times 10^{-4}$ |

| Relative Permeability Parameters | |
|---|---|
| $k_{rw}$ | $0.9S^3$ |
| $k_{ro}$ | $0.9(1-S)^2$ |
| $S_{wi}$ | 0.1 |
| $S_{or}$ | 0.1 |

| Model Specification | 1D | 2D |
|---|---|---|
| Model dimensions (length/width) | 10/3 | 1 |
| Gridblocks | 10 | 10 x 10 |
| Injection/production rate (PV/timestep) | 0.0137 | 0.0137(average) |
| Number of data per well | 60 | 60 |

| Case | Dimensions | Parameters Estimated | Number of Parameters | Initial Guesses of Parameters |
|---|---|---|---|---|
| 1 | 1 | Step function of $k$* | 9 | $k = 0.2$ darcy |
| 2 | 1 | Sine function of $\phi$** | 10 | $\phi = 0.18$ |
| 3 | 1 | $k$(step function), $\phi$(sine function) | 19 | $k = 0.2$ darcy, $\phi = 0.18$ |
| 4 | 1 | $k$, $\phi$, $k_r$ (1 zone) | 11 | $k = 0.05$ darcy, $\phi = 0.2$‡ |

*Table 1: Specification of Waterflood Cases*

(Source: P.H. Yang and A.T. Watson, 1988[4])

Only three cases will be studied since only the first three cases involved the gradient based method that related to this project.

Case 1: The permeability was approximated in the inverse space where the parameter approximated was the inverse of the permeability. The permeability inverse parameter space can produce a more stable and precise second-order estimation of the performance index.

Case 2: The porosity values were set as unknown parameters of each grid block. A sine function defined the true porosities.
Case 3: The nine harmonic-average values of the porosity and absolute permeability values of all ten grid blocks were set to be unknown.

The Root Mean Squared Error (RMSE) values for each case of all four methods are shown in Table 2. RMSE were computed separately for porosity and permeability due to different in scales.

| Case | Algorithm* | RMSE** (%) $k$ | RMSE** (%) $\phi$ |
|---|---|---|---|
| 1 | BFGS | 1.34 | |
| | SSVM | 0.98 | |
| | Steepest descent† | 14.58 | |
| | Conjugate gradient | 1.34 | |
| 2 | BFGS | | 0.52 |
| | SSVM | | 0.40 |
| | Steepest descent† | | 5.48 |
| | Conjugate gradient | | 0.47 |
| 3 | BFGS | 2.72 | 2.23 |
| | SSVM | 2.59 | 2.00 |
| | Conjugate gradient‡ | 19.33 | 20.51 |

*Table 2: Accuracy of Estimates for Waterflood Cases*

(Source: P.H. Yang and A.T. Watson, 1988[4])

Precise outcomes were achieved by BFGS and SSVM methods in Cases 1, 2 and 3 referring to Table 2 where the RMSE values for permeability and porosity were smaller than 3 %. While steepest descent and conjugate gradient have large RMSE for all cases compared to BFGS and SSVM.

Figure 12, 13 and 14 illustrates the plot of performance indices standardized by the initial of the performance index vs. work equivalents for Cases 1, 2 and 3.

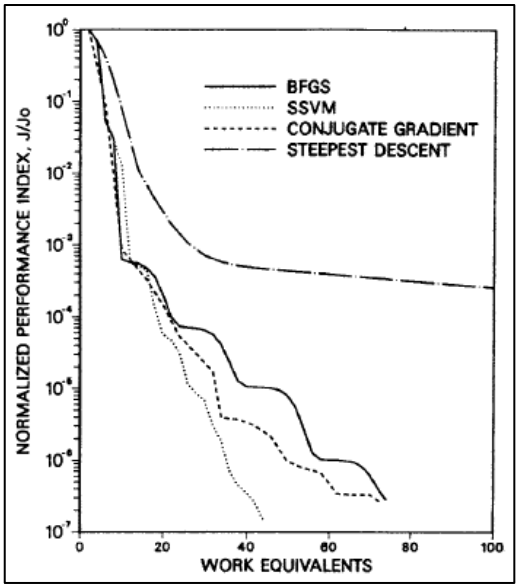


*Figure 12: Decrease in performance index vs. work equivalents for Case 1.*

(Source: P.H. Yang and A.T. Watson, 1988[4])

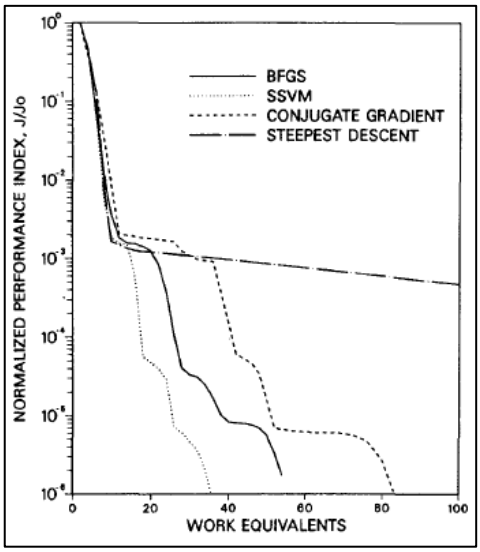


*Figure 13: Decrease in performance index vs. work equivalents for Case 2.*

(Source: P.H. Yang and A.T. Watson, 1988[5])

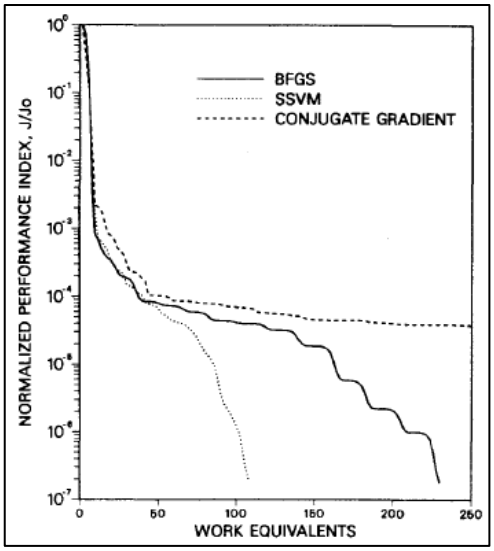


*Figure 14: Decrease in performance index vs. work equivalents for Case 3.*

(Source: P.H. Yang and A.T. Watson, 1988[5])

Performances of both SSVM and BFGS methods are more excellent than steepest-descent method. Moreover based on Table 2, BFGS and SSVM provide nearly magnitude perfection in the parameter estimates precision compared to steepest descent. This precision is basically unreachable for steepest descent referring the convergence rate presented by steepest descent in Figure 12 and 13. SSVM method can be concluded as more effective than BFGS method in all three cases, which it requires 30 to 55% lesser work equivalents compared to BFGS method based on Figure 12, 13 and 14.

Precise outcomes were also gained from conjugate-gradient method in Cases 1 and 2. For Case 1, the conjugate gradient method conducted well where the performance index is closely quadratic in the unknown parameters even though it was not as effective as SSVM method. For Case 2 in Figure 13, conjugate-gradient method turn out less effective and need 55 % greater work equivalents than the BFGS method since the performance index was not as quadratic as in Case 1. Based on Figure 14 for Case 3, it was much more complex function of unknown parameters compared to Cases 1 and 2 where the conjugate-gradient method accomplished very deficiently and unsuccessful to converge.

As a conclusion from the results achieved, variable-metric methods would be better choice for water flood cases in updating the parameters in history matching. The steepest -descent method has weakness in progressing very slowly in the minimum vicinity, while the conjugate gradient methods shown to be less efficient than variable-metric methods in both numerical tests and theoretical parts.

## 3.7 Kalman Filter for History Matching

Kalman filter is a traditional method for model calibration and data assimilation that has been widely and successfully implemented. Zhang, D., H. Li, and H. Chang [16] approached estimation of non-Gaussian permeability field by applying a probabilistic collocation based Kalman filter (PCKF). The probabilistic collocation method is applied to solve the coefficient of polynomial chaos development. Probabilistic collocation technique is a non-invasive to the reservoir model hence it permits the forward simulations to be implemented independently with current reservoir simulators, as in Monte Carlo simulation. In the study, they compared the effectiveness, accurateness and applicability between PCKF and ensemble Kalman filter (EnKF) which both of these methods can estimate non-Gaussian permeability field accurately.

### Case Studies

They provide samples to assess the PCKF performance for history matching purpose by considering a synthetic two-dimensional reservoir model. The problem is five-spot water flooding where the reservoir is divided to 50x50 grid blocks evenly. Four producers are placed around the corners and one injector is placed at the center. The injector is set with constant water injection rate of 3000 stb/day and with maximum bottom hole pressure (BHP) of 10000 psi. All four producers are assumed to have a constant 2000 psi BHP. The observations of producer's oil production rate (OPR) and water cut (WCT) and injector's BHP are accessible every 50 days until 1000 days. The relative error of the observations is assumed to be 5%. Figure below shows the implementation workflow of PCKF for non-Gaussian random field k(x).

The estimation is implemented for two different permeability field of non-Gaussian field. The first case is using the permeability field that has a right-skewed probability density distribution (PDF).

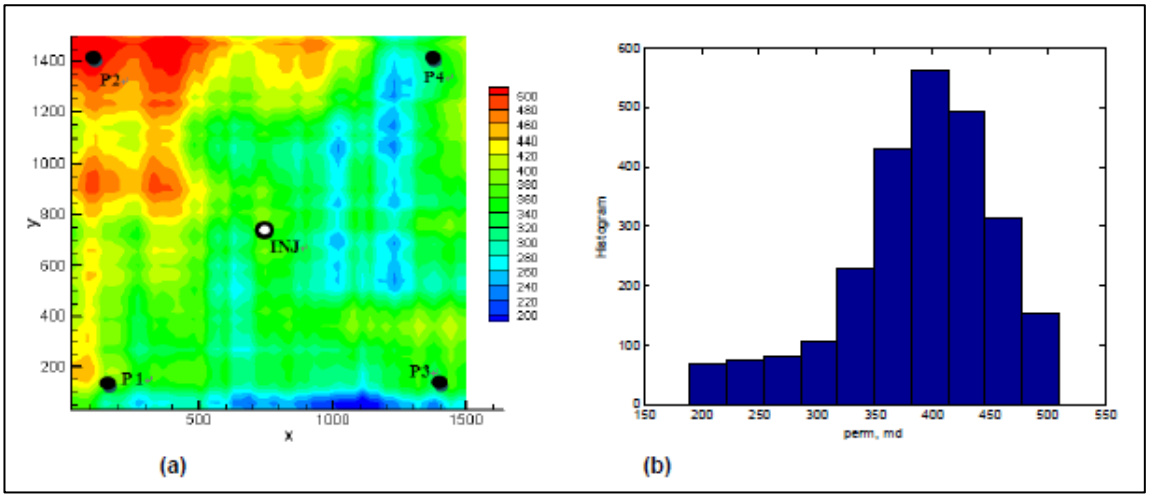


*Figure 15: (a) The reservoir configuration and reference permeability field for case 1. (b) Permeability field histogram for case 1.*

(Source: Zhang, D., H. Li, and H. Chang, 2011 [16])

Figure 16 (a) represents the approximated mean of permeability field of PCKF while figure 16 (b) and (c) represent the estimated for two different EnKF runs. The reference field in Figure 15 (a) displays a large high permeability area in the upper left corner. Hence PCKF estimate catches this major pattern of permeability field, certain small fluctuations are disregards and there is an unpredicted area with higher permeability close to the right side. In contrast, the two EnKF runs estimation are unalike and both of them are unsuccessful to capture the major patterns of the reference permeability field.

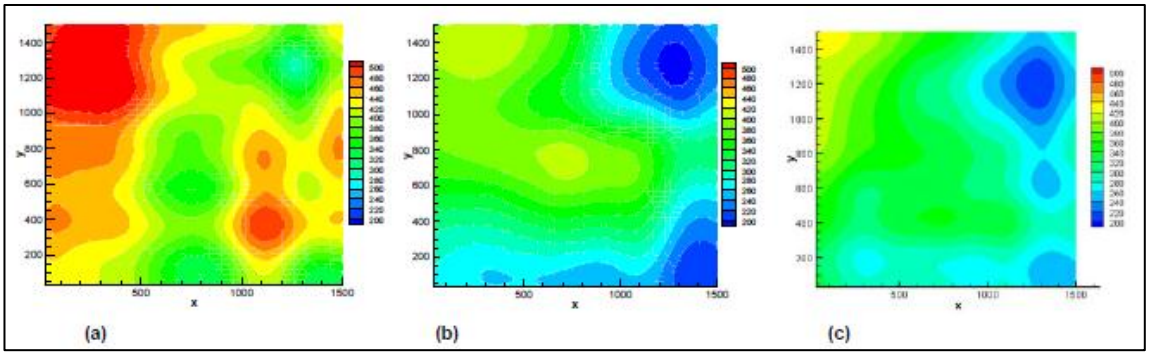


*Figure 16: Mean estimate of permeability field. (a) PCKF; (b) EnKF 1 and (c) EnKF 2.*

(Source: Zhang, D., H. Li, and H. Chang, 2011 [16]

For the second case, the permeability field of another non-Gaussian PDF is estimated where the permeability is left-skewed with higher skewness than the first case. Shown below in Figure 17 is the reference permeability field and permeability field histogram for case 2.The reservoir configurations and the 86 of ensemble size for each run in PCKF and EnKF remain the same for the second case.

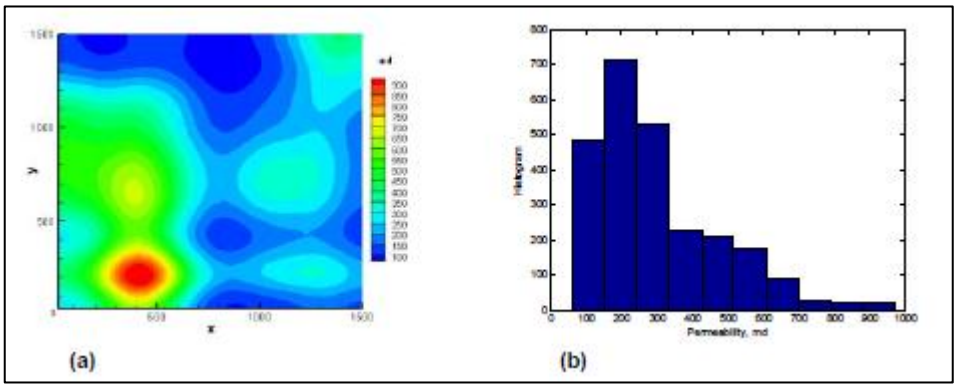


*Figure 17: (a) Reference permeability field for case 2; (b) Permeability field histogram for case 2.*

(Source: Zhang, D., H. Li, and H. Chang, 2011 [16])

Figure 18 shows the mean estimate of permeability field obtained from PCKF and form two runs of EnKF. It can be seen that the mean estimate of PCKF is much closer to the reference permeability field compared to EnKF since the pattern of the contour map matches the reference. This shows that the estimated values of PCKF are at same level as the reference with high accuracy and efficiency.

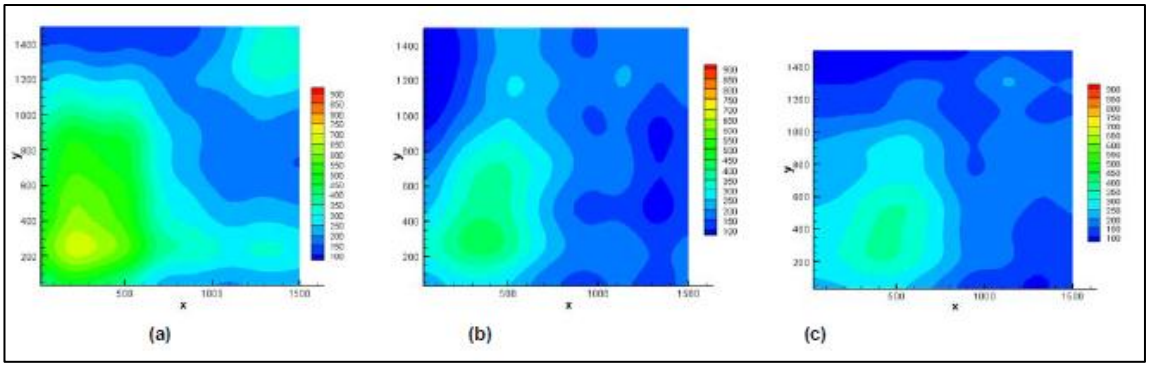


*Figure 18: Mean estimate of permeability field. (a) PCKF; (b) EnKF 1 and (c) EnKF 2.*

(Source: Zhang, D., H. Li, and H. Chang, 2011 [16])

In order to further investigating the estimated permeability field accuracy, root mean square (RMSE) is obtained. Figure 19 below demonstrates the RMSE of estimated permeability from PCKF and two run of EnKF. It can generally be seen that PCKF has lesser RMSE than bot of EnKF runs. RMSE from PCKF declines with time meaning that as more observations are assimilated, the permeability estimation becomes closer to the reference and the uncertainties are very low compared to EnKF.

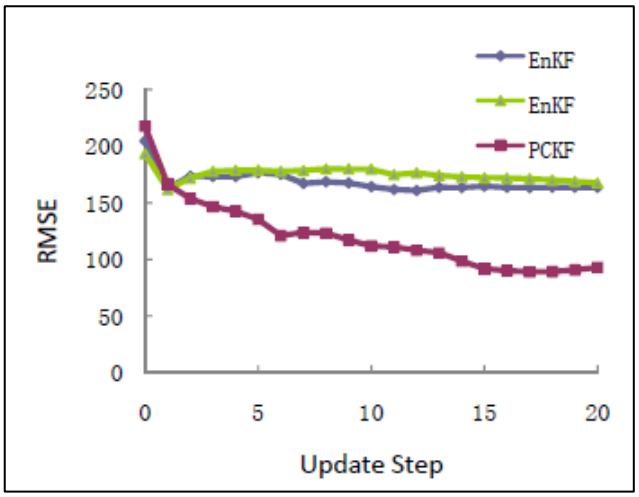


*Figure 19: RMSE of permeability estimation vs. update step. Comparison between PCKF and two different runs of EnKF.*

(Source: Zhang, D., H. Li, and H. Chang, 2011 [16])

As a conclusion from the results achieved, PCKF outperforms the EnKF in terms of the accuracy and efficiency in permeability field estimation and the prediction after estimation.

# CHAPTER 4

# METHODOLOGY

## 4.1 Research Methodology

The research methodology for this project is analyzing Kalman filter and steepest descent methods for the assisted history matching purpose. The methodology is applied by following the process flow illustrated in project activities section of this report.

## 4.2 Software Used

### 4.2.1 ECLIPSE

For this project, ECLIPSE is used to simulate two sets of reservoir parameters in order to obtain the historical and simulated model. In the real situation by following the history matching procedure, this reservoir flow simulator also should be used to predict the parameters after been updated using MATLAB.

### 4.2.2 MATLAB

MATLAB is not used for this research project but if both methods are practically applied for the history matching purpose hence it should be used to update the reservoir parameters after been predicted by ECLIPSE and this process will loops until the objective function or error calculated is minimized.

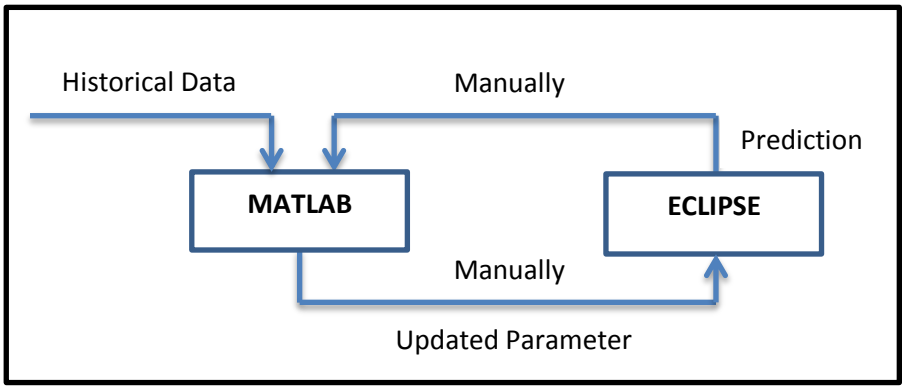


*Figure 20 Process Flow of MATLAB and ECLIPSE*

Figure 20 is the process flow of application of MATLAB and ECLIPSE for this project. The parameters will be updated manually by using MATLAB and send the information to the ECLIPSE to predict the parameters. Then, the historical data and the predicted data will be combined into the MATLAB using both Kalman filter and steepest descent methods to continue the process of updating the parameters. The assisted history matching technique is a semi-automatic system and that is the reason of updating and predicting the parameters manually as shown in the figure above.

## 4.3 Project Activities

Figure 21 shows the methodology of this project.

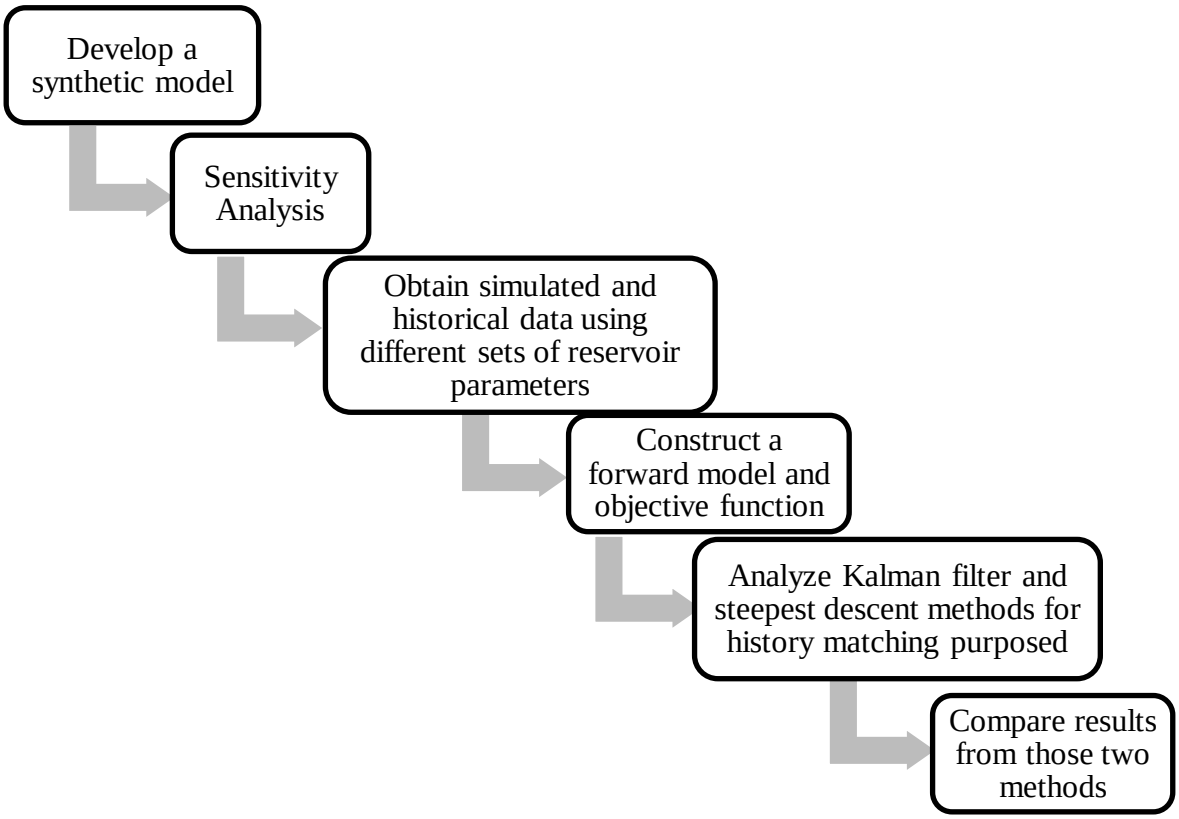


*Figure 21: Methodology*

### 4.3.1 Synthetic Model

According to the McGraw-Hill Dictionary of Scientific and Technical Terms, synthetic data are any production data valid to a specified condition that are not acquired by direct measurement. Synthetic data is applied in many fields as information's filter to keep the confidentiality of certain aspects of the data. It is generated to meet particular requirements or certain circumstances that may not be found in the original or real data. It can be beneficial when designing any kind of system because the synthetic data are used as a theoretical or simulation value. This enables to prepare for the solution if obtain any unexpected or unsatisfactory results. Synthetic data are often created to symbolize the authentic data and permits a baseline to be set. Hence for this project, a synthetic model is built based on ODEH model which is a most commonly used synthetic model for reservoir application. The details of the synthetic model will be discussed later in Chapter 6.

### 4.3.2 Sensitivity Analysis

Sensitivity analysis is one of the important procedure need to be investigated in order to choose which reservoir model parameters that we are going to test and update. Hence, two sensitivity analysis are conducted which are in terms of permeability and porosity. Figure 22 below shows the sensitivity analysis for permeability where the changes in permeability for each zones in each layers of the reservoir did affect the production rate perfectly. The permeability of the grid blocks is set to be different between all three layers by having four zones at each of the layer, hence produce twelve different permeability. This factor also is one of the reasons in increasing the sensitivity due to the variation of permeability.

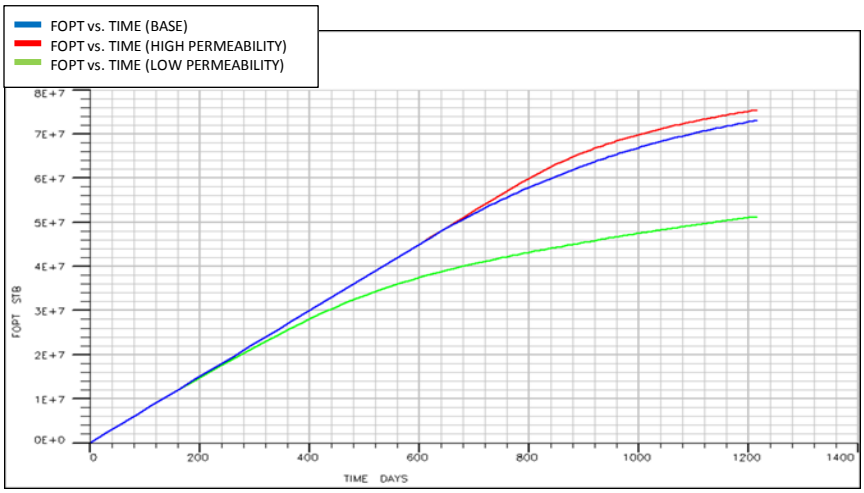


*Figure 22: Sensitivity Analysis for Permeability*

Figure 23 below is the sensitivity analysis for porosity it also affect the production rate but the changes is too much. Even with slight changes in the porosity did affect a lot in the production rate hence it is not a good selection for parameters updating. As conclusion on the sensitivity analysis, variation on permeability is sensitive and good enough to affect the production rate of the well.

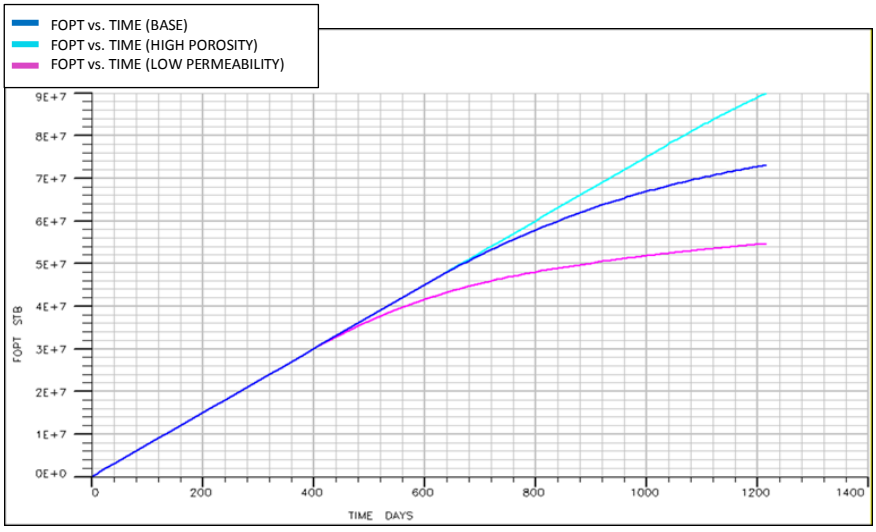


*Figure 23: Sensitivity Analysis for Porosity*

### 4.3.3 Simulated and Historical Data

Historical and simulated data are obtained from two different sets of reservoir parameters. Both of the sets are differed from its permeability value where simulated data has higher permeability compared to historical data. Permeability is chosen as interest parameter based on sensitivity analysis that has been conducted shown in Chapter 6.

### 4.3.4 Fluid Flow in Reservoir (Forward Model)

Mass balance equation and Darcy equation are some of the equations required to develop the forward model. Figure 24 below shows a one dimensional slab of porous material as a picture of the material balance equation where to illustrate the mass accumulation inside a porous material. Forward model is constructed to develop ECLIPSE by using the pressure equation.

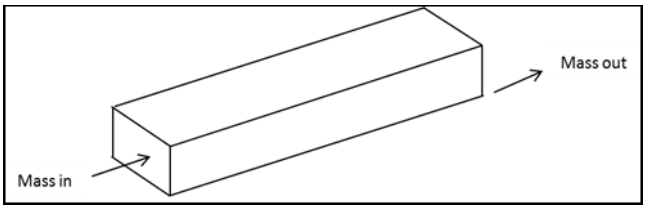


*Figure 24: One dimensional slab of porous material*

For this study, forward model is constructed for one-dimensional flow for vertical well of two phase fluid flow. These derivations come from Darcy's equation, continuity equation, and compressibility descriptions for fluid and rock, predicting constant viscosity and vary permeability. Here are the simple equations, include transient fluid flow inside the reservoir.

Firstly, by considering a simple slab of porous material, a mass balance equation can be expressed as Equation (7):

$$\left\lfloor \begin{matrix} Mass\ into \\ the\ element \end{matrix} \right\rfloor - \left\lfloor \begin{matrix} Mass\ out\ of \\ the\ element \end{matrix} \right\rfloor = \left\lfloor \begin{matrix} Rate\ of\ change\ of\ mass \\ inside\ the\ element \end{matrix} \right\rfloor \quad (7)$$

For constant cross sectional area, the conservation mass or continuity equation of two phases, one-dimensional flow can simplifies to Equation (8) and (9):

$$\text{Oil: } -\frac{d}{dx}(\rho_o u_o) + \frac{d}{dy}(\rho_o u_o) = \frac{d}{dt}(\emptyset \rho_o S_o) \quad (8)$$

$$\text{Water: } -\frac{d}{dx}(\rho_w u_w) + \frac{d}{dy}(\rho_w u_w) = \frac{d}{dt}(\emptyset \rho_w S_w) \quad (9)$$

For the left hand side, Darcy equation is substituted while formation volume factor, B is substituted, and density $\rho$ is cancelled into the continuity equations for both sides for each phase.

$$\text{Oil: } \frac{d}{dx}\left(\frac{kk_{ro}}{\mu_o \beta_o}\frac{dP_o}{dx}\right) - q_o = \frac{d}{dt}\left(\frac{\emptyset S_o}{\beta_o}\right) \quad (10)$$

$$\text{Water: } \frac{d}{dx}\left(\frac{kk_{rw}}{\mu_w \beta_w}\frac{dP_w}{dx}\right) - q_o = \frac{d}{dt}\left(\frac{\emptyset S_w}{\beta_w}\right) \quad (11)$$

Discretization of Flow Equation

Forward:

$$\left[f(x)\frac{dP_l}{dx}\right]_{i+1/2} = \left[f(x)\frac{dP_l}{dx}\right]_i + \frac{\Delta x_{i/2}}{1!}\frac{d}{dx}\left[f(x)\frac{dP_l}{dx}\right]_i + \frac{\left(\Delta x_{\frac{i}{2}}\right)^2}{2!}\frac{d^2}{d^2x}\left[f(x)\frac{dP_l}{dx}\right]_i \quad (12)$$

Backward:

$$\left[f(x)\frac{dP_l}{dx}\right]_{i-1/2} = \left[f(x)\frac{dP_l}{dx}\right]_i + -\frac{\Delta x_{i/2}}{1!}\frac{d}{dx}\left[f(x)\frac{dP_l}{dx}\right]_i + \frac{\left(-\Delta x_{\frac{i}{2}}\right)^2}{2!}\frac{d^2}{d^2x}\left[f(x)\frac{dP_l}{dx}\right]_i \quad (13)$$

Where,

$$\left(\frac{dPl}{dx}\right)_{i+1/2} = \frac{Pl_{i+1} - Pl_i}{\Delta x} \tag{14}$$

$$\left(\frac{dPl}{dx}\right)_{i-1/2} = \frac{Pl_i - Pl_{i-1}}{\Delta x} \tag{15}$$

Hence, by subtracting the forward and backward equation and substituting the above equation into the forward and backward equation, the result is:

$$\frac{d}{dx}\left[f(x)\frac{dP_l}{dx}\right] = \frac{f(x)_{i+1/2}\frac{P_{i+1}-P_i}{\Delta x} - f(x)_{i-1/2}\frac{P_i - P_{i-1}}{\Delta x}}{\Delta x} \tag{16}$$

Oil: $\frac{d}{dx}\left(\frac{kk_{ro}}{\mu_o B_o}\frac{dP_o}{dx}\right)_i \approx T_{xoi+\frac{1}{2}}(P_{oi+1} - P_{oi}) + T_{xoi-\frac{1}{2}}(P_{oi-1} - P_{oi})$ (17)

Water: $\frac{d}{dx}\left(\frac{kk_{rw}}{\mu_w B_w}\frac{dP_w}{dx}\right)_i \approx T_{xwi+\frac{1}{2}}(P_{wi+1} - P_{wi}) + T_{xwi-\frac{1}{2}}(P_{wi-1} - P_{wi})$ (18)

Where,

$$T_{xoi+\frac{1}{2}} = \frac{2\lambda_{oi+1/2}}{\Delta x\left(\frac{\Delta x}{k_{i+1}} + \frac{\Delta x}{k_i}\right)} \tag{19}$$

For the right hand side, the equation after the time discretization can be expressed by using chain rule and substituting the rock compressibility, Cr in the equation.

Oil: $\frac{d}{dt}\left(\frac{\emptyset}{\beta_o}\right)_i = \frac{\emptyset_i}{\Delta t_{oi}}\left[\frac{Cr}{\beta_o} + \frac{d(1/\beta_o)}{dP_o}\right]_i (P_o^{t+\Delta t} - P_{oi}^t)$ (20)

Standard backward approximation of time derivative

$$\left(\frac{\emptyset}{B_o}\frac{dS_o}{dt}\right)_i \approx -\frac{\emptyset_i}{B_{oi}\Delta t_i}(S_{wi}^{t+\Delta t} - S_{wi}^t) \tag{21}$$

$$\frac{d}{dt}\left(\frac{\emptyset S_o}{B_{oi}}\right)_i \approx C_{poq}\left(P_{oi}^{t+\Delta t} - P_{oi}^t\right) + C_{swoi}(S_{wi}^{t+\Delta t} - S_{wi}^t) \tag{22}$$

Where,

$$C_{poq} = \frac{\emptyset(1-S_{wi})}{\Delta t}\left[\frac{c_r}{B_o} + \frac{d\left(\frac{1}{B_o}\right)}{dP_o}\right]_i \quad (23)$$

$$C_{swoi} = -\frac{\emptyset_i}{B_{oi}\Delta t_i} \quad (24)$$

While for water,

$$\text{Water: } \frac{d}{dt}\left(\frac{\emptyset S_w}{B_w}\right) = \frac{\emptyset}{B_w}\frac{dS_w}{dt} + S_w\frac{d}{dt}\left(\frac{\emptyset}{B_w}\right) \quad (25)$$

$$\frac{d}{dt}\left(\frac{\emptyset}{B_w}\right) = \frac{d}{dP_w}\left(\frac{\emptyset}{B_w}\right)\frac{dP_w}{dt} = \frac{d}{dP_w}\left(\frac{\emptyset}{B_w}\right)\left(\frac{dP_o}{dt} - \frac{dP_{cow}}{dt}\right) \quad (26)$$

$$\frac{d}{dt}\left(\frac{\emptyset S_w}{B_w}\right)_i \approx C_{powi}\left(P_{oi}^{t+\Delta t} - P_{oi}^{t}\right) + C_{swwi}(S_{wi}^{t+\Delta t} - S_{wi}^{t}) \quad (27)$$

Where,

$$C_{powi} = \frac{\emptyset_i S_{wi}}{\Delta t}\left[\frac{c_r}{B_o} + \frac{d\left(\frac{1}{B_w}\right)}{dP_w}\right]_i \quad (28)$$

$$C_{swwi} = \frac{\emptyset_i}{B_{wi}\Delta t_i} - \left(\frac{dP_{cow}}{dS_w}\right)_i C_{powi} \quad (29)$$

In the following, linear flow equations are solved mathematically by using normal finite difference estimation for both derivative terms$\frac{\partial^2 P}{\partial x^2}$ and$\frac{\partial P}{\partial T}$ . Firstly, the x-coordinate must be split into a number of discrete grid blocks, while the time coordinate must be separated into discrete time steps. Next, the pressure in every block can be solved for mathematically for every time step. The discretization of the flow equations for both left and right hand side produce:

Oil:

$$T_{xoi+\frac{1}{2}}(P_{oi+1} - P_{oi}) + T_{xoi-\frac{1}{2}}(P_{oi-1} - P_{oi}) - \acute{q}_{oi} = C_{poq}\left(P_{oi}^{t+\Delta t} - P_{oi}^{t}\right) + C_{swoi}(S_{wi}^{t+\Delta t} - S_{wi}^{t}) \quad (30)$$

Water:

$$T_{xwi+\frac{1}{2}}[(P_{wi+1}-P_{wi})-(P_{cowi+1}-P_{cowi})]+T_{xwi-\frac{1}{2}}[(P_{wi-1}-P_{wi})-(P_{cowi-1}-P_{cowi})]-\acute{q}_{wi}=C_{powi}\left(P_{oi}^{t+\Delta t}-P_{oi}^{t}\right)+C_{swwi}(S_{wi}^{t+\Delta t}-S_{wi}^{t}) \quad (31)$$

Where,

$$T_{xoi+\frac{1}{2}}=\frac{2\lambda_{oi+1/2}}{\Delta x\left(\frac{\Delta x}{k_{i+1}}+\frac{\Delta x}{k_i}\right)} \quad (32)$$

$$T_{xoi-\frac{1}{2}}=\frac{2\lambda_{oi-1/2}}{\Delta x\left(\frac{\Delta x}{k_{i-1}}+\frac{\Delta x}{k_i}\right)} \quad (33)$$

$$T_{xwi+\frac{1}{2}}=\frac{2\lambda_{wi+1/2}}{\Delta x\left(\frac{\Delta x}{k_{i+1}}+\frac{\Delta x}{k_i}\right)} \quad (34)$$

$$T_{xwi-\frac{1}{2}}=\frac{2\lambda_{wi-1/2}}{\Delta x\left(\frac{\Delta x}{k_{i+1}}+\frac{\Delta x}{k_i}\right)} \quad (35)$$

Combine the discrete form of oil and water by eliminating the saturation of water terms and arrange the equations.

$$P_{oi-1}\left(T_{xoi-\frac{1}{2}}^{t}+\alpha_i T_{xoi-\frac{1}{2}}^{t}\right)+P_{oi}\left(-\left(T_{xoi+\frac{1}{2}}^{t}+T_{xoi-\frac{1}{2}}^{t}+C_{poq}^{t}\right)-\alpha_i\left(T_{xwi+\frac{1}{2}}^{t}+T_{xwi-\frac{1}{2}}^{t}+C_{powi}^{t}\right)\right)+P_{oi+1}\left(T_{xoi+\frac{1}{2}}^{t}+\alpha_i T_{xwi+\frac{1}{2}}^{t}\right)=-\left(C_{pooi}^{t}+\alpha_i C_{powi}^{t}\right)P_{oi}^{t}+\acute{q}_{oi}+\alpha_i\acute{q}_{wi}+\alpha_i T_{xwi+\frac{1}{2}}^{t}(P_{cowi+1}-P_{cowi})^{t}+\alpha_i T_{xwi-\frac{1}{2}}^{t}(P_{cowi-1}-P_{cowi})^{t} \quad (36)$$

The general pressure equation may be written as Equation (37):

$$a_i P_{oi-1}+b_i P_{oi}+c_i P_{oi-1}=d_i \quad (37)$$

Where,

$$a_i=T_{xoi-\frac{1}{2}}^{t}+\alpha_i T_{xoi-\frac{1}{2}}^{t} \quad (38)$$

$$b_i=-\left(T_{xoi+\frac{1}{2}}^{t}+T_{xoi-\frac{1}{2}}^{t}+C_{poq}^{t}\right)-\alpha_i\left(T_{xwi+\frac{1}{2}}^{t}+T_{xwi-\frac{1}{2}}^{t}+C_{powi}^{t}\right) \quad (39)$$

$$c_i=T_{xoi+\frac{1}{2}}^{t}+\alpha_i T_{xwi+\frac{1}{2}}^{t} \quad (40)$$

$$d_i = -\left(C^t_{pooi} + \alpha_i C^t_{powi}\right)P^t_{oi} + \acute{q}_{oi} + \alpha_i \acute{q}_{wi} + \alpha_i T^t_{xwi+\frac{1}{2}}(P_{cowi+1} - P_{cowi})^t + \alpha_i T^t_{xwi-\frac{1}{2}}(P_{cowi-1} - P_{cowi})^t \quad (41)$$

From the equation, $\alpha = -\frac{C^t_{swwi}}{C^t_{swoi}}$ (42)

Consider the boundary conditions for production at bottom hole pressure specified well condition where:

$$q_{oı} = \frac{WC_ı}{A\Delta x}\acute{\lambda_{oı}}(P_{oı} - P_{bhı}) \quad (43) \qquad q_{wi} = \frac{WC_i}{A\Delta x}\lambda_{wi}(P_{wi} - P_{bhi}) \quad (44)$$

After substitute the boundary condition into the equation, the equation can be expressed as:

$$P_{oi-1}\left(T^t_{xoi-\frac{1}{2}} + \alpha_i T^t_{xoi-\frac{1}{2}}\right) + P_{oi}\left(-\left(T^t_{xoi+\frac{1}{2}} + T^t_{xoi-\frac{1}{2}} + C^t_{poq} + \frac{WC_i}{A\Delta x}\lambda_{oi}\right) - \alpha_i\left(T^t_{xwi+\frac{1}{2}} + T^t_{xwi-\frac{1}{2}} + C^t_{powi} + \frac{WC_i}{A\Delta x}\lambda_{wi}\right)\right) + P_{oi+1}\left(T^t_{xoi+\frac{1}{2}} + \alpha_i T^t_{xwi+\frac{1}{2}}\right) = -\left(C^t_{pooi} + \alpha_i C^t_{powi}\right)P^t_{oi} - \frac{WC_i}{A\Delta x}\lambda_{oi}P_{bhi} - \alpha_i\frac{WC_i}{A\Delta x}\lambda_{wi}P_{bhi} + \alpha_i T^t_{xwi+\frac{1}{2}}(P_{cowi+1} - P_{cowi})^t + \alpha_i T^t_{xwi-\frac{1}{2}}(P_{cowi-1} - P_{cowi})^t \quad (45)$$

Where,

$$a_i = T^t_{xoi-\frac{1}{2}} + \alpha_i T^t_{xoi-\frac{1}{2}} \quad (46)$$

$$b_i = -\left(T^t_{xoi+\frac{1}{2}} + T^t_{xoi-\frac{1}{2}} + C^t_{poq} + \frac{WC_i}{A\Delta x}\lambda_{oi}\right) - \alpha_i\left(T^t_{xwi+\frac{1}{2}} + T^t_{xwi-\frac{1}{2}} + C^t_{powi} + \frac{WC_i}{A\Delta x}\lambda_{wi}\right) \quad (47)$$

$$c_i = T^t_{xoi+\frac{1}{2}} + \alpha_i T^t_{xwi+\frac{1}{2}} \quad (48)$$

$$d_i = -\left(C^t_{pooi} + \alpha_i C^t_{powi}\right)P^t_{oi} - \frac{WC_i}{A\Delta x}\lambda_{oi}P_{bhi} - \alpha_i\frac{WC_i}{A\Delta x}\lambda_{wi}P_{bhi} + \alpha_i T^t_{xwi+\frac{1}{2}}(P_{cowi+1} - P_{cowi})^t + \alpha_i T^t_{xwi-\frac{1}{2}}(P_{cowi-1} - P_{cowi})^t \quad (49)$$

This equation is generalized in order to be run using the MATLAB to get the simulated parameters.

**Objective Function**

According to [15] the meaning of objective function based on the accessible observed variable, and is described as the quantity of difference within observation data such as field pressure, reservoir production historical data, seismic survey, and the simulator response parameters. It is required to identify the gap between the simulated and observed data correlated to each parameter involved in the procedure. Based on [6] there are three common formulas to compute the objective function:

Least-square formulation:

$$F = (d^{obs} - d^{cal})^T (d^{obs} - d^{cal}) \quad (50)$$

Weighted least-square formulation:

$$F = (d^{obs} - d^{cal})^T w(d^{obs} - d^{cal}) \quad (51)$$

Generalized least-square formulation:

$$F = \frac{1}{2}(1 - ß)\left\{\left(d^{obs} - d^{cal}\right)^T C_d^{-1}\left(d^{obs} - d^{cal}\right)\right\} + \frac{1}{2}ß\left\{\left(a - a_{prior}\right)^T C_a^{-1}\left(a - a_{prior}\right)\right\} \quad (52)$$

From the formula, $d^{obs}$ denotes the observed data, $d^{cal}$ represents the response of the coordination, as estimated from the forward modeling, while w is a diagonal matrix that allocates weights to the measurement. The weights of every well and each data type are allocated as a function of the available data points number in a set, also on the uncertainty connected within every sort of measurement. The β is a weighting factor that indicates the relative strength of the original model while Cd symbolizes the data covariance matrix; Cd delivers correlation information between the data. Cα is the parameter covariance matrix of the mathematical model. Since the correlations among observed data are challenging to assess, only the diagonal terms are normally considered in the covariance matrices.

### 4.3.5 Analyze Methods

Afterward, Kalman filter and steepest descent methods are analyzed in the next chapter in order to understand the procedure of applying those methods to the assisted history matching.

### 4.3.6 Compare the results

Finally, both methods are compared. This is the main objective of this project which to compare the results between the Kalman filter and steepest descent methods for assisted history matching. By comparing both methods, the results will proved which method will be the best method to be applied in the history matching.

### 4.4 Project Timeline (Gantt chart)

Table 3 shows the project timeline for each of the tasks.

| NO | ACTIVITIES | MAY | | JUNE | | | | JULY | | | | AUGUST | | | | SEPT |
|---|---|---|---|---|---|---|---|---|---|---|---|---|---|---|---|---|
| | | **W1** | **W2** | **W3** | **W4** | **W5** | **W6** | **W7** | **W8** | **W9** | **W10** | **W11** | **W12** | **W13** | **W14** | **W15** |
| 1 | Analyze and study the Kalman filter and steepest descent methods | | | | | | | | | | | | | | | |
| 4 | Submission of Progress Report | | | | | | | | | | | | | | | |
| 5 | Analyze both methods for assisted history matching | | | | | | | | | | | | | | | |
| 6 | Comparative Analysis | | | | | | | | | | | | | | | |
| 7 | PRE SEDEX | | | | | | | | | | | | | | | |
| 8 | Submission of Draft Final Report | | | | | | | | | | | | | | | |
| 9 | SEDEX | | | | | | | | | | | | | | | |
| 10 | Submission of Dissertation (Soft Bound) | | | | | | | | | | | | | | | |
| 11 | Submission of Technical Paper | | | | | | | | | | | | | | | |
| 12 | VIVA | | | | | | | | | | | | | | | |
| 13 | Submission of Dissertation (Hard Bound) | | | | | | | | | | | | | | | |

*Table 3 : Gant Chart*

## 4.5 Key Milestone

Table 4 shows the completion of each of the project activities.

| No | Activities | Completion week |
|---|---|---|
| 1 | Completion of Progress Report | Week 8 |
| 2 | Completion of Comparative Analysis | Week 9 |
| 3 | Completion of PRE SEDEX | Week 10 |
| 4 | Completion of SEDEX | Week 11 |
| 5 | Completion of Technical Paper | Week 13 |
| 6 | Completion of Final Report (Soft Copy) | Week 13 |
| 7 | Completion of VIVA | Week 15 |
| 8 | Completion of Final Report (Hard Bound ) | Week 15 |

*Table 4 Key Milestone*

# CHAPTER 5

# STEEPEST DESCENT & KALMAN FILTER

## 5.1 Steepest Descent

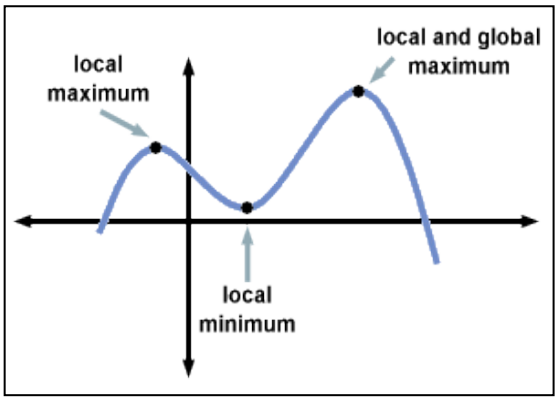


*Figure 26: Local maximum and minimum*

(Source: Spark Notes, 2014)

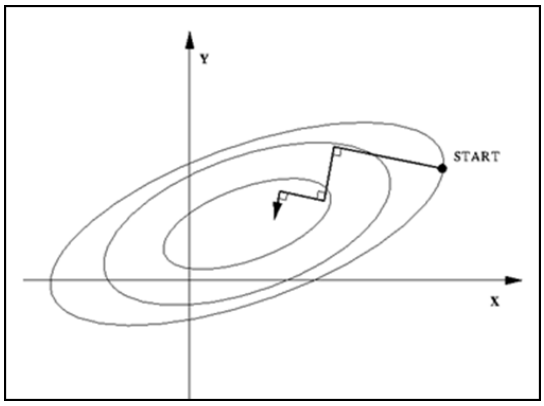


*Figure 25 Method of Steepest Descent*

(Source: Trond Hjorteland, 1999)

In accordance to Xu Wang [17], steepest descent is a simplest gradient methods using a function F(x) that can be determined and differentiated between a specified boundary in order to search the local minimum of F(x). As shown in Figure 26, F(x) can be obtained by simply picking an arbitrary point$x_o$within the range of the function and gradually moving down the gradient towards the minimum in a zig-zag manner, until it converges to the definite point. Local minimum as illustrated in Figure 25 is the value of a function at the lowest point of a curve in a graph. In the paper, it stated that steepest descent is very easy to implement, simple and fast in each iteration. Referring to a paper with title "Method of Steepest Descent", the paper shows a very simple example and clear picture on steepest descent, also the methods to solve the minimization problem along a line regarding this method. However, the author concludes that steepest descent is a bad choice for the optimization problem even though it is easy to apply and very stable method.

## 5.2 Implementation of Steepest Descent

Furthermore, A. T. Watson and W. J. Lee [18] presenting a new process for production or well test data of automatic history matching. The performance of the algorithm is evaluated by history matching then the Gauss-Newton and steepest descent algorithms are compared. This algorithm has been modified from the Marquardt-Lavenberg method to attain better strength and productivity for automatic history matching. The results shows it is very effective for the case that they studied, compared to Gauss-Newton and steepest descent.

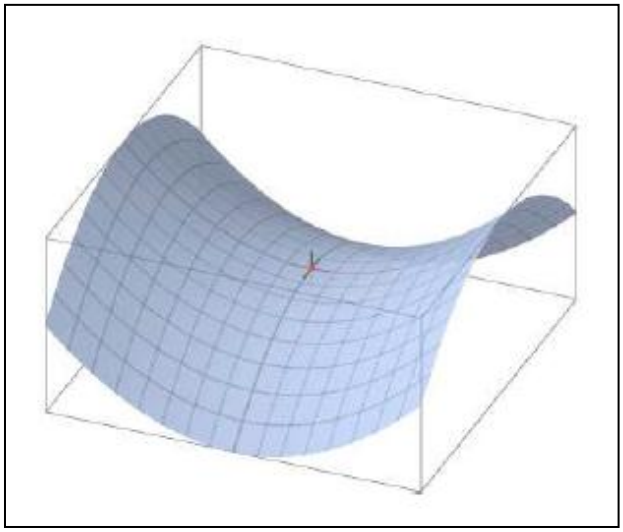

*Figure 27 Saddle Point*

(Source: Xu Wang, 2008 [17])

According to Xu Wang [17], there are many useful applications of steepest descent method. One of them is applying the method for a complex interval in order to find the saddle point. Figure 27 above shows the saddle point where the surface represent a saddle that bend up in one direction and bend down in a other direction. Regarding the contour lines, a saddle point can be identified by a contour that performs to intersect itself. On the other hand, Soonhong Cheong [19] presented the applications of steepest descent to calculate source-independent waveform inversion using normalized wavefield by convolution. For calculation of the steepest descent of the new objective function, they utilize a matrix formalism initiated from the Green's function symmetry of wave computation. For this application, they compute the steepest descent without explicitly

calculating the Jacobian matrix. In another application, Taegong Seo and Changsoo Shin [20] stated that steepest descent is applied in order to create source-independent waveform inversion algorithm. In contrast to application mentioned before, this paper apply backpropagation algorithm of reverse time migration, thus completely calculating the steepest descent by matching backpropagated residuals with simulated source. Lastly in their conclusion, they compare their method with the algorithm explicitly calculating the Jacobian matrix, the backpropagation based algorithm attain computational proficiently in the source situation.

### 5.3 Demonstration of Steepest Descent

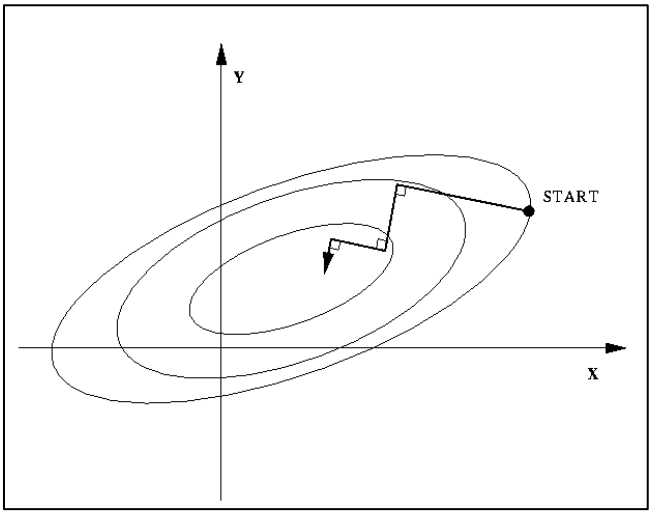


*Figure 28 Steepest Descent approaches the minimum in a zig-zag pattern, where the new search direction is orthogonal to the previous.*

(Source: Trond Hjorteland, 1999)

Steepest Descent is the simplest gradient methods. The direction chosen is when f declines most rapidly, which is in opposite direction from $\nabla f(x_i)$ as shown in Figure 28. The search begins at an arbitrary point $x_0$, then move down the gradient, until it is close enough to the solution. The iterative process is shown in the equation:

$$x_{k+1} = x_k - \lambda_k \nabla f(x_k) = x_k - \lambda_k g(x_k) \tag{53}$$

Where $g(x_k)$ is the gradient at one point. $\lambda_k$ is the step taken in the chosen direction. The direction should move to the point with minimum value of function f, which is zero directional derivatives. The directional derivative is:

$$\frac{d}{d\lambda_k} f(x_{k+1}) = \nabla f(x_{k+1})^T . \frac{d}{d\lambda_k} x_{k+1} = -\nabla f(x_{k+1})^T . g(x_k) \quad (54)$$

Setting this equation to zero, it can be seen that $\lambda_k$ should be chosen to make $\nabla f(x_{k+1})$ and $g(x_k)$ are orthogonal to each other. Next step is taken in the negative gradient direction of this new point and will get a zig-zag manner as demonstrated in Figure 12. When the extremum is determined within a selected accuracy$\epsilon$, the iteration can be stop.

There is actually a minimization issue along a line, where the line is produced by first expression for different values of $\lambda_k$. It is commonly solved by searching a minimum point along a line or called linear search. Thus, the search for a minimum of f(x) is decreased to linear searches sequence. This Steepest Descent implementation is regularly referred as the optimal gradient method. The iterative algorithms by Steepest Descent Method, using a linear search are as shown below.

| | |
|---|---|
| Initializing $g_0 = \nabla f(x_0), d_0 = -g_0$ | (55) |
| $\Delta$ Determine the step length $\lambda_k$: min f$(x_k + \lambda_k d_k)$ | (56) |
| Calculate the new point: $x_{k+1} = x_k + \lambda_k d_k$ | (57) |
| Calculate the gradient: $g_{k+1} = \nabla$f$(x_{k+1})$ | (58) |
| Set direction of search: $d_{k+1} = -g_{k+1}$ | (59) |

Alternatively, this method can begin with a chosen $\lambda_k$ value, which will be improved during the iterations, to ensure that the function declines at each iteration. This is simpler, and works better, for a difficult linear search calculation. There might be more iteration to reach the minimum, but each iteration will take lesser time compared to linear search.

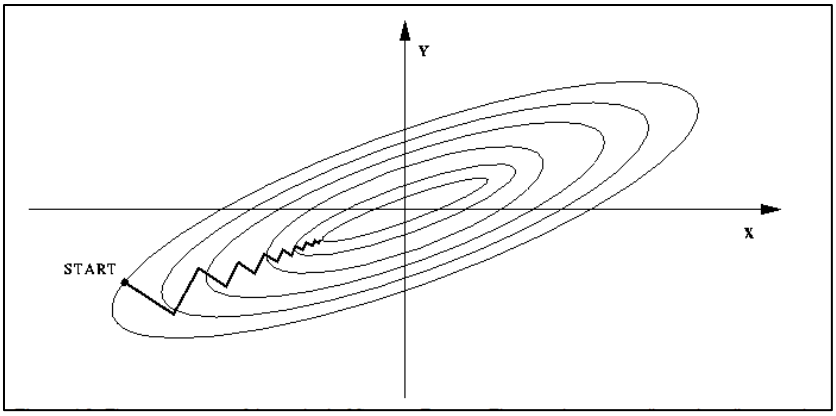


*Figure 29: The convergence of the method of Steepest Descent. The step size is continuously getting smaller, crossing the valley, as it close the minimum*

(Source: Trond Hjorteland, 1999)

The method of Steepest Descent is simple, easy to implement, and each of the iteration is fast. It is very stable as if the minimum point exists, the method will definitely to locate them at least an infinite number of iterations. While on the other side of steepest descent, it normally has slow convergence. A system might end up spending an infinite number of iterations before discovering a minimum point. It begins with a realistic convergence, but the progress will get slower as approaching the minimum. It is proved in Figure 29, in quadratic function with a long and narrow valley case. The technique may converge fast for bad scaled structures, but it depends on a good choice of initial point. It can be said that the Steepest Descent method can be applied when the minimum has been indicated, yet is commonly considered as a bad choice for any optimization problem. It is normally used only in combination with other optimizing techniques.

## 5.4 Kalman filter

Regarding Faragher, R. [21], the Kalman filter is more than 50 years old but it stays as one of the most essential and well-known data fusion algorithms until today. Named from Rudolf E. Kalman, the prominent success of the Kalman filter is because of its minor computational constraint, well-designed recursive properties, and its position as the ideal estimator for 1D linear system using Gaussian error statistics. Normal applications of Kalman filter comprise smoothing noisy data and contributing approximations of interest parameters. In other source, Welch, G. and Bishop, G.[22]

stated that Kalman filter provides a proficient recursive solution of the least-squares technique, same as mentioned by some of other authors. He also mentioned that the filter is very strong in numerous features where it provides predictions of previous, current, and future conditions even though when the specific nature of the modeled structure is unknown. They studied the discrete Kalman filter which has been widely implemented in autonomous or assisted navigation area. On the other hand, regarding [8], Kalman filter is one of the important toolbox of mathematical tools that can be used for stochastic approximation from noisy sensor measurements. Maybeck, P.S. [23] reported that Kalman filter is an ideal recursive data processing system where it incorporates all information that can be provided regardless of their precision. Recursive in Kalman filter means it is not necessary to keep all previous data in storage and processes every time a new measurement taken. It process all existing measurements to approximate the present value of the variable by using information of the system, the statistical report of the system noises or measurement errors and any available data for initial conditions of the interest variable.

According to Oliver D.S, et al [24] in their paper, the most basic method for the data assimilation for linear problem is the Kalman filter and it is called recursive method. The second recursive method discussed by the authors is the extended Kalman filter as an adaptation for nonlinear problems. Lastly, the ensemble Kalman filter (EnKF) method is introduced as a feasible alternative to classical recursive methods and to traditional history matching. Their review claimed that ensemble Kalman filter (EnKF) contributes the greatest approximation of the population mean and the ensemble produces an experiential approximation of the probability density. By using this method, it is unnecessary to linearize the dynamical equation or the relationship between state variables and the data, also to compute and update the estimate of the covariance. However, Sigurd I. Aanonsen, et al [25] stated the disadvantages of using ensemble Kalman filter (EnKF). They mentioned that during the reservoir simulation models, the problems with this method are raised in the low standard demonstration of the ideal covariance matrix, robust nonlinearities in the mathematical model, non-Gaussian prior representations and the implementation to huge-scale field simulations. EnKF is argued not producing a correct estimate of the posterior probability distribution.

## 5.5 Implementation of Kalman Filter

Kalman filter is one of the filter algorithm that is widely implemented in many industry because of it practicality and robustness. According to Welch, G and Bishop, G. [8], the Kalman filter has been implemented comprehensively for tracking in collaborating computer graphics. They used a single constraint Kalman filter in their HiBall Tracking System which is commercially accessible from 3rdTech. The filter has also been used for multi-sensor fusion in the marketable Constellation™ wide area tracking system by Intersense, also for motion estimation.

On the other point of view, Faragher, R. [21] claimed that Kalman filter is one of the most famous and widespread data fusion algorithms in the field of information processing. The most popular primary implementation of the Kalman filter was when Neil Armstrong went to the moon by the Apollo navigation computer and he was successfully back to earth safely. Nowadays, Kalman filters are working in satellite navigation tool, smart phones, and computer games. Other applications include smoothing the output from laptop track pads, phase locked loops in radio appliance, global positioning system receivers and others. It is a great achievement when Kalman filter is implemented in a very wide area especially in petroleum industry, for instance, history matching where it helps for parameter estimation by estimating undefined parameters such as permeability, saturation, porosity and pressure from indirect measurement.

Regarding Kelly, A. [26], the filter formulation of Kalman filter is fairly general. This generality is conceivable because the problem has been attended in 3-Dimensional, in state space with an improved state vector, asynchronously and with tensor calculus measurement models. He also mentioned that the filter has wide ranging implementation include map matching in mapping applications, as overall integration and dead reckoning component when Inertial Navigation System (INS) or Global Positioning System (GPS) is used and as the base of an automobile location estimation system.

## 5.6 Demonstration of Kalman Filter

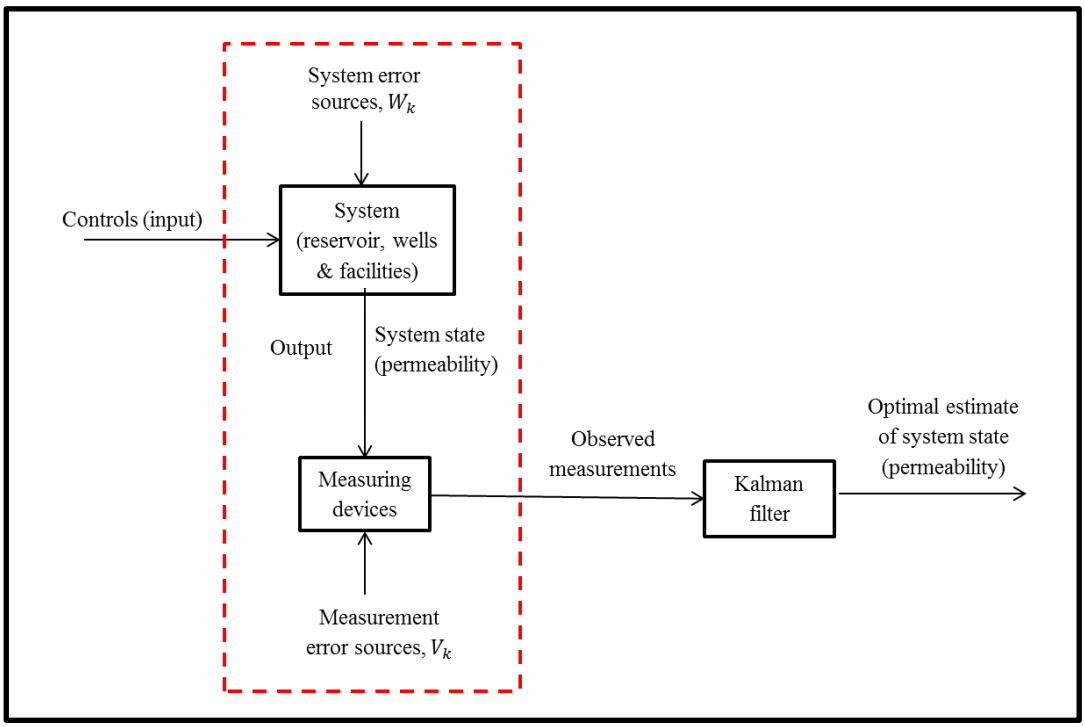


*Figure 30 Typical Kalman filter application*

(Source: Peter S. Maybeck, 1979[23])

Figure 30 shows a normal situation how Kalman filter could be applied advantageously. It is a system that determined by identified controls and measuring tools provides the value of definite relevant measures. Information of these structure inputs and outputs is clearly obtainable from the physical structure for approximation process. The necessity of the filter now becomes clear.

Based on the theoretical perspective, Kalman filter is a process allowing precise implication in linear dynamical structure, Bayesian model which alike to Markov model but where the state space of the latent variables is constant and which entire latent and observed variables have a Gaussian distribution.

The Kalman filter is normally derived using vector algebra as a minimum mean squared estimator. The applications of a Kalman filter are numerous for example tracking objects, economics, navigation and many computer vision applications.

1) **System descriptions (Build a model)**

The Kalman filter model predicts that the state of a system during time t developed from the prior state at time t-1 according to the equation (60):

$$x_k = Ax_{k-1} + w_k \tag{60}$$

- $x_k$ is a state vector of the system at current ($k^{th}$) time where for this project, it is the permeability.
- A is the system dynamics matrix which applies the outcome of every system state parameter during time t-1 on the system state at time t.
- $W_k$ is the model error which is error comes from eliminating the right hand side of discretization of flow equation during generating forward model.

Measurements of the system can be achieved, regarding to the model:

$$z_k = Hx_k + v_k \tag{61}$$

- $z_k$ is the measurement vector.
- H is the measurement matrix.
- $v_k$ is the measurement error which occur during the calculation.

2) **Time Update**

3) **Measurement Update**

Figure 31 below shows that Kalman filter has two different stages as part of each cycle.

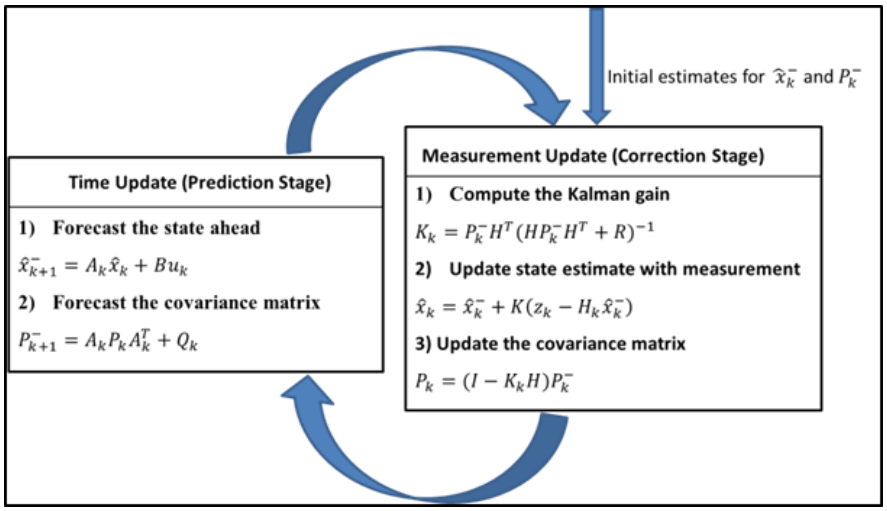


*Figure 31 The discrete Kalman filter cycle [22]*

Here the two stages of prediction and filtering (or updating) are demonstrated. For the Kalman filter, the initial estimate for the state ($\hat{x}_0$) and the state covariance ($P_0$) is required together with the model error and measurement covariance (respectively Q and R). These variables are needed to tune the Kalman filter response. If the initial state and the state covariance are near to its real value, then the settling time will normally be shorter. Both the measurement covariance and the model error covariance adjust the Kalman gain $K_k$. If the measurement covariance is big it means that there is a lot of error in the measurement. Consequently, the Kalman gain will be lesser and the observed result of the analysis step will decrease. When the model error covariance is huge, the Kalman gain will be greater and will have a stronger impact from the analysis step. These two tuning parameters have to be measured together and finally the ratio between them needs to be noted.

**Example**

The example is to try estimating a scalar random constant, such as permeability measurement from a source. It is assumed that it has a constant value of **a**mD (millidarcy), and has some noise readings above and below **a**mD. It is assumed that the standard deviation of the measurement noise, R is 10mD.

Firstly, need to build the model:

$$x_k = Ax_{k-1} + w_k \quad = x_{k-1} + w_k \tag{62}$$

$$z_k = Hx_k + v_k \quad = x_k + v_k \tag{63}$$

The equation is reduced to a very simple form because it is an example for one dimensional problem, so it is a numerical value instead of matrix form. Since the signal is a continuous value, the constant A can be assumed as 1 because it is known that the next value will be the same as previous one. The value of H is also 1 because the measurement is collected of the state value and several noise.

Here in Table 5 are the assumed measurement values:

| Time (ms) | 1 | 2 | 3 | 4 | 5 | 6 | 7 | 8 | 9 | 10 |
|---|---|---|---|---|---|---|---|---|---|---|
| Value (mD) | 390 | 500 | 480 | 290 | 250 | 320 | 340 | 480 | 410 | 450 |

*Table 5 Time vs Value*

The initial value of k is assumed as 0, $x_0 = 0$ and $P_0 = 1$. If $P_0$ is chosen as 0, it means that there is no noise at the surroundings and this theory will cause all $\hat{x}_k$ to be 0. Here in Table 6 are the equations for the time update and measurement update.

| **Time Update (prediction)** | **Measurement Update (correction)** |
|---|---|
| $\hat{x}_k^- = \hat{x}_{k-1}$ (64) | $K_k = \frac{P_k^-}{P_k^- + R}$ (66) |
| $P_k^- = P_{k-1}$ (65) | $\hat{x}_k = \hat{x}_k^- + K_k(z_k - \hat{x}_k^-)$ (67) |
| | $P_k = (I - K_k H)P_k^-$ (68) |

*Table 6 Equations of Time Update and Measurement Update*

Next, value of $\hat{x}_k$ is calculated for each iteration in Table 7.

| k (ms) | $z_k$ | $\hat{x}_{k-1}$ | $P_k^-$ | Time Update | Measurement Update |
|---|---|---|---|---|---|
| 1 | 390 | 0 | 1 | $\hat{x}_1^- = \hat{x}_{k-1} = 0$<br>$P_1^- = P_{k-1} = 1$ | $K_1 = \frac{P_k^-}{P_k^- + R} = 0.0909$<br>$\hat{x}_1 = \hat{x}_k^- + K_k(z_k - \hat{x}_k^-)$<br>$= 35.45$<br>$P_1 = (I - K_k H)P_k^- = 0.9091$ |
| 2 | 500 | 35.45 | 0.9091 | $\hat{x}_2^- = 35.45$<br>$P_2^- = 0.9091$ | $K_2 = 0.0833$<br>$\hat{x}_2 = 74.15$<br>$P_2 = 0.833$ |
| 3 | 480 | 74.15 | 0.833 | $\hat{x}_3^- = 74.15$<br>$P_3^- = 0.833$ | $K_3 = 0.0769$<br>$\hat{x}_3 = 105.36$<br>$P_3 = 0.769$ |
| 4 | 290 | 105.36 | 0.7692 | $\hat{x}_4^- = 105.36$<br>$P_4^- = 0.7692$ | $K_4 = 0.07143$<br>$\hat{x}_4 = 118.54$<br>$P_4 = 0.7143$ |
| 5 | 250 | 118.54 | 0.7143 | $\hat{x}_5^- = 118.54$<br>$P_5^- = 0.7143$ | $K_5 = 0.0667$<br>$\hat{x}_5 = 127.35$<br>$P_5 = 0.667$ |
| 6 | 320 | 127.35 | 0.667 | $\hat{x}_6^- = 127.35$<br>$P_6^- = 0.667$ | $K_6 = 0.0625$<br>$\hat{x}_6 = 139.39$<br>$P_6 = 0.625$ |
| 7 | 340 | 139.39 | 0.625 | $\hat{x}_7^- = 139.39$<br>$P_7^- = 0.625$ | $K_7 = 0.0588$<br>$\hat{x}_7 = 151.19$<br>$P_7 = 0.588$ |
| 8 | 480 | 151.19 | 0.588 | $\hat{x}_8^- = 151.19$<br>$P_8^- = 0.588$ | $K_8 = 0.0555$<br>$\hat{x}_8 = 169.44$<br>$P_8 = 0.555$ |
| 9 | 410 | 169.44 | 0.555 | $\hat{x}_9^- = 169.44$<br>$P_9^- = 0.555$ | $K_9 = 0.0526$<br>$\hat{x}_9 = 182.09$ |

| | | | | | |
|---|---|---|---|---|---|
| | | | | | $P_9 = 0.526$ |
| 10 | 450 | 182.09 | 0.526 | $\hat{x}_{10}^{-} = 182.09$<br>$P_{10}^{-} = 0.526$ | $K_{10} = 0.0500$<br>$\hat{x}_{10} = 195.49$<br>$P_{10} = 0.500$ |

*Table 7 List of iterations*

These numerical values can be completed via a computer algorithm which is the appropriate solution. By writing the algorithm, it can be found that Kalman filter is very easy to implement. Figure 32 below shows that Kalman filter algorithm converges to the true permeability value. This example is only for 10 iterations, but in more iteration, it will converge even better.

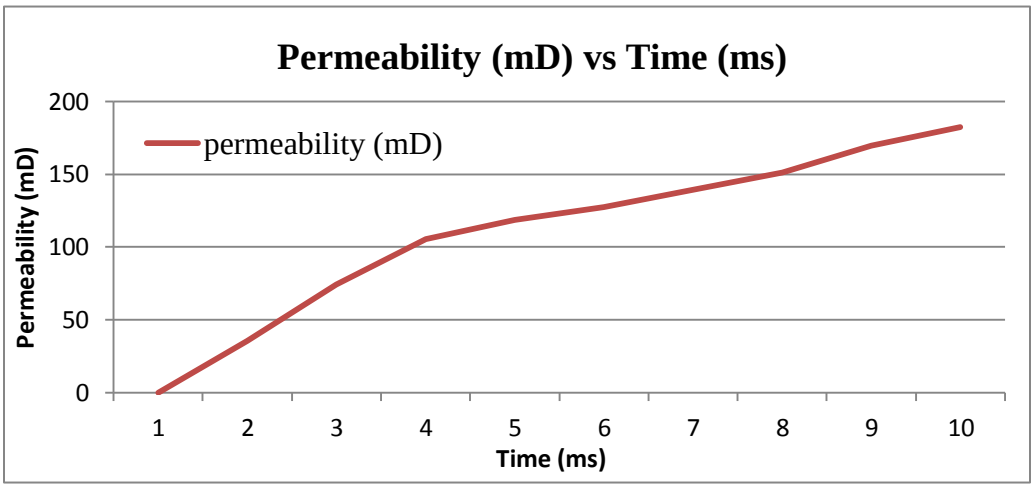


*Figure 32 Permeability Graph*

To enable the convergence in less iteration, the important thing is to:

- Model the system more elegantly
- Estimate the noise more precisely

# CHAPTER 6

# RESULT AND DISCUSSION

After completed with the synthetic model, historical and simulated data are obtained. The historical and simulated curve is illustrated in figure below in FOPT (Field oil production cumulative total) graph, FOPR (Field Oil Production Rate) graph, WBHP (Well bottom hole pressure) graph and WGOR (Well gas oil ratio) graph. Referring to figure 33 and 34, it can be seen there is a gap between historical and simulated curve. Hence, by applying both of the optimization methods to the assisted history matching, a new red curves which is the expected updated model is added in the FOPT and FOPR graphs shown below parallel to the purpose of history matching which to obtain a good model that closer to the historical model for the forecasting purposes.

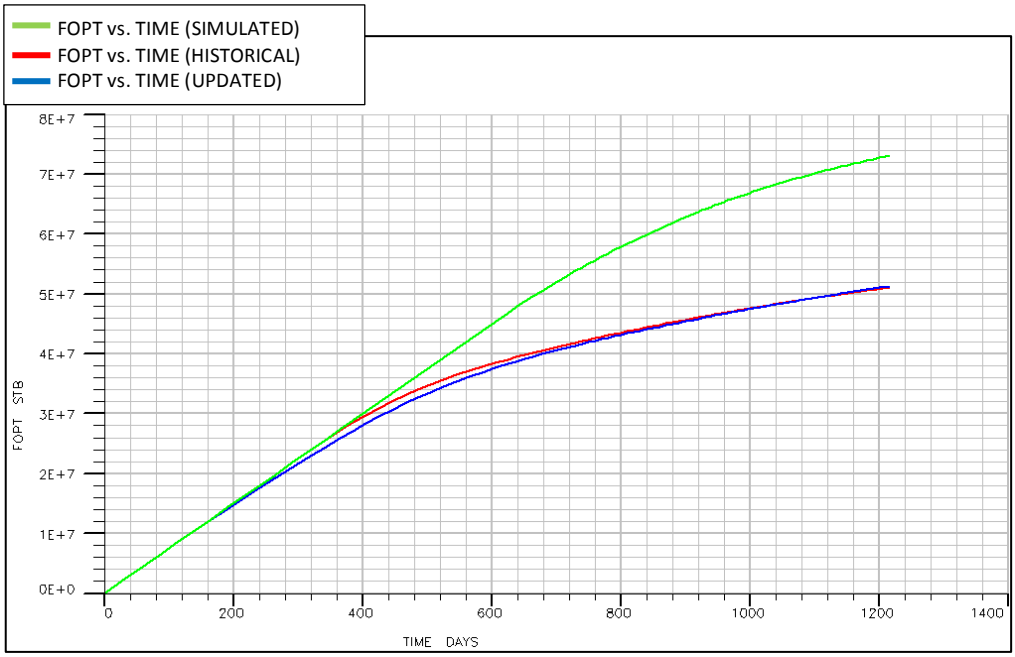


*Figure 33: FOPT (Field oil production cumulative total) vs. Time (Days)*

Figure 34 below shows that the production rate starts at 75000STB/Day and constantly producing hydrocarbon until certain time where the production rate is dropped. The

green curve which symbolizes the production rate of simulated model is started to decrease at 600$^{th}$ days while the blue curve which denotes the production rate of historical model decrease earlier than the simulated model. This happened due to difference in permeability where simulated model has higher permeability than the historical model. Higher permeability will cause higher in production rate and it has been proven in this graph.

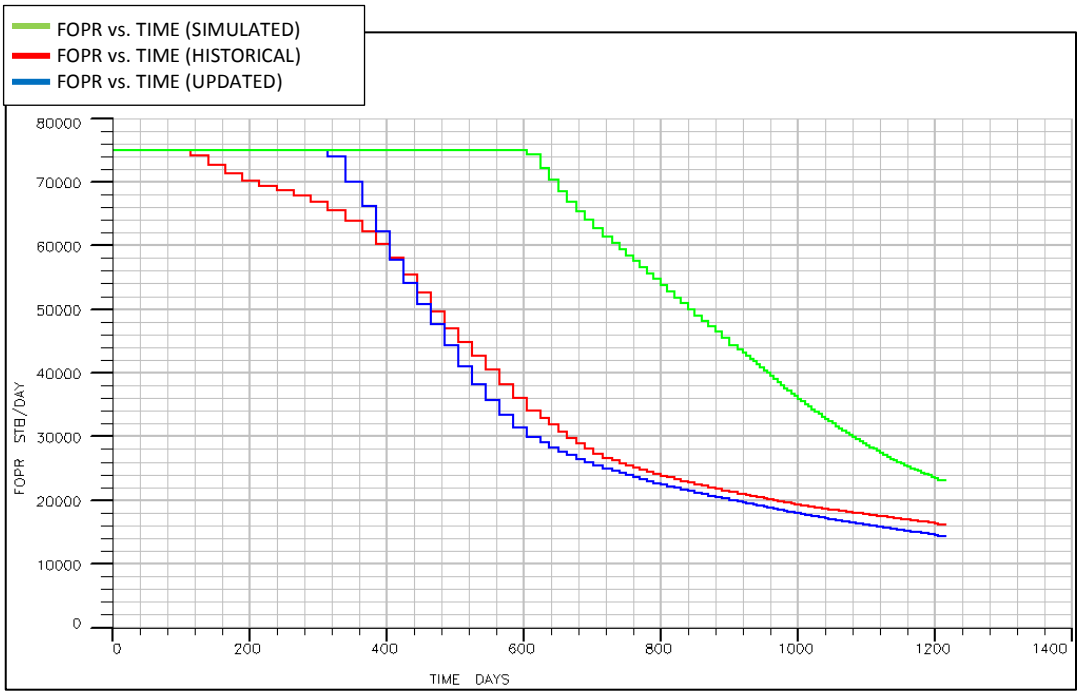


*Figure 34: FOPR (Field Oil Production Rate) vs. Time (Days)*

Referring to figure 35 below, as bottom hole pressure (BHP) of these model is set as constant, hence the BHP for both historical and simulated starts to get constant at 120$^{th}$ days and 640$^{th}$ days respectively. BHP usually will start from a higher value then decrease as the hydrocarbon started to flow through the bottom hole towards the pipeline. We can see the relationship between FOPR and WBHP graph where when the BHP start to decrease or constant, the production rate also will start to drop. This is because when the pressure to push the hydrocarbon is decreasing, the production flowrate will be affected as it will also decreasing.

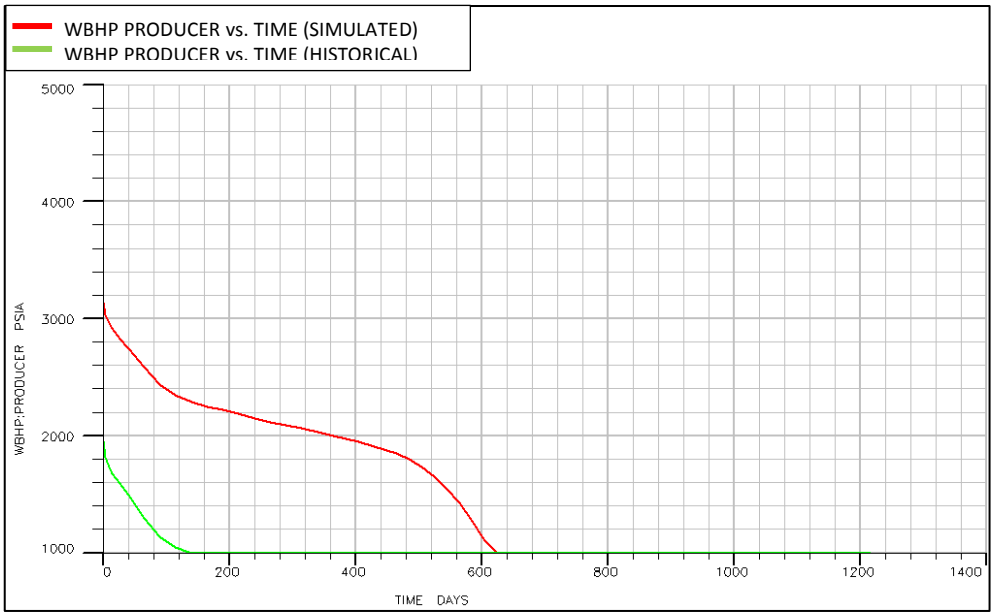


*Figure 35: WBHP (Well bottom hole pressure) vs. Time (Days)*

According to figure 36, the gas oil ratio (GOR) of simulated model increasing more rapidly compared to historical model.

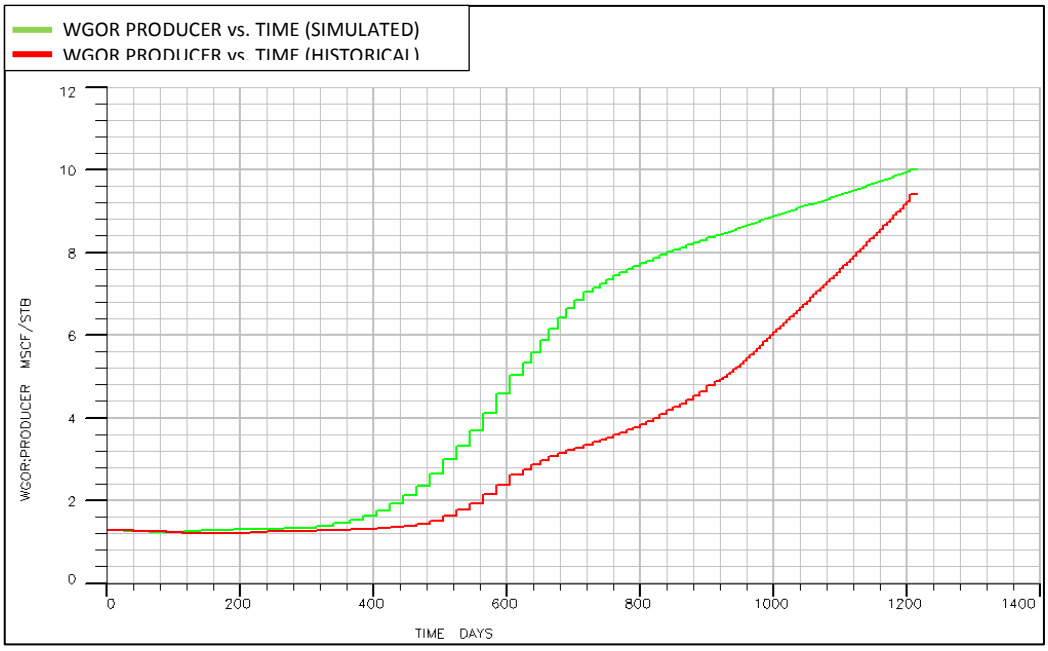


*Figure 36: WGOR (Well gas oil ratio) vs. Time (Days)*

## 6.1 Synthetic Model

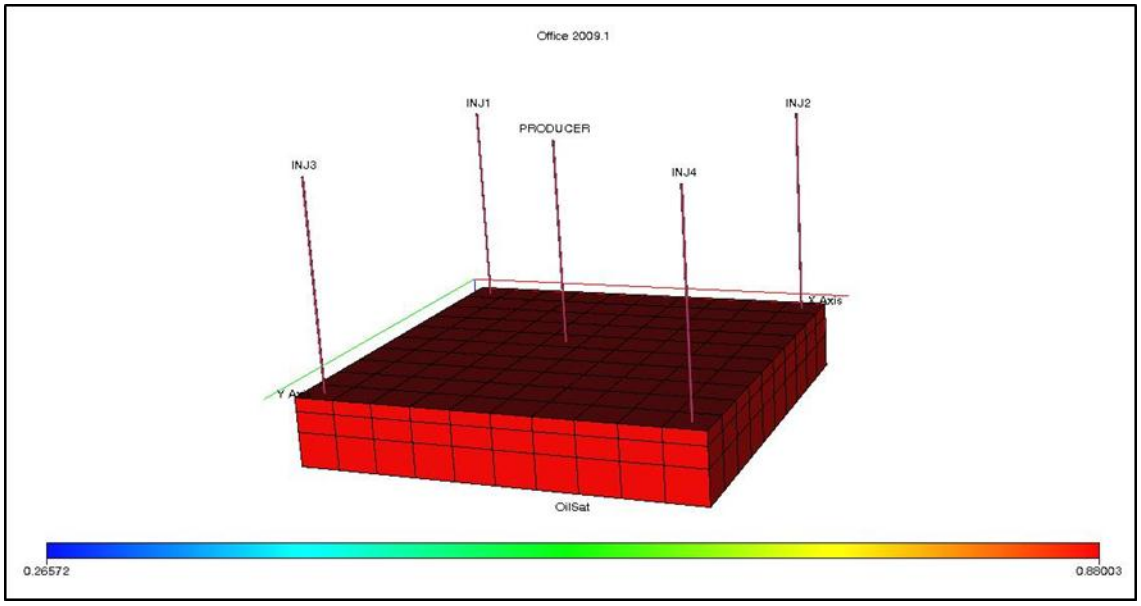


*Figure 37: Synthetic Model*

Figure 37 above shows the synthetic model built from ODEH model which has a very close character with real reservoir and most commonly synthetic data used for history matching purpose and also for other applications. The data from ODEH model such as the saturation, porosity, viscosity and others is used in order to extract some of the reservoir parameters to build a new synthetic model.

This model illustrates a 10x10x3 grid block. The x-axis of this model is 1000 ft, the y-axis is 1000ft and the z-axis has three layers with thickness of 20 ft, 30 ft and 50 ft respectively. There are four injector wells at location (1, 1), (10, 1), (1, 10) and (10, 10). The producing well is only one which is at (5, 5). Both producer well and injection wells are producing hydrocarbon and injecting gas at third layer. The reason of injecting gas is to reduce the density of fluid and viscosity of fluid, hence increase the flowrate, This is because the gas bubble will cause the fluid lighter. Gas injection also can increase pressure, thus push the hydrocarbon upward and increase the production of the

hydrocarbon. The bottom hole pressure (BHP) of this model is set to be constant in order to acquire different production rate.

This synthetic model is divided into twelve zones of permeability where there are four zones for each layer. For the first layer, the range of the zone is (1 5 1 5 1 1), (6 10 1 5 1 1), (1 5 6 10 1 1) and (6 10 6 10 1 1). At the second layer, the four permeability zone is at (1 5 1 5 2 2), (6 10 1 5 2 2), (1 5 6 10 2 2) and (6 10 6 10 2 2). Lastly at the third layer, the different permeability zone is at (1 5 1 5 3 3), (6 10 1 5 3 3), (1 5 6 10 3 3) and (6 10 6 10 3 3). The permeability is set at twelve different zones in order to analyze the sensitivity of the permeability changes in two different sets of reservoir parameters data. The permeability of simulated model is set higher compared to historical model. The reason is to analyze the sensitivity due to the permeability.

## 6.2 Historical model and Simulated Model

Here is the process of obtaining the historical and simulated synthetic data:

### 6.2.1 Historical

Historical model is built based on ODEH synthetic model by changing some of the reservoir parameters. The permeability of this historical model is set randomly between 250 to 1500 which are increasing from first layer to third layer. Figures 38-41 show the 3 dimension (3D) of historical model at different time to illustrate the changing of oil saturation along the time. The oil saturation shows the existence of oil, water and gas in the reservoir. Red color refers to oil and blue color refer to gas as it can be seen that in 1984, there are a lot of gas at the first layer due to the four injection well that inject gas at each of the edge of the grid blocks.

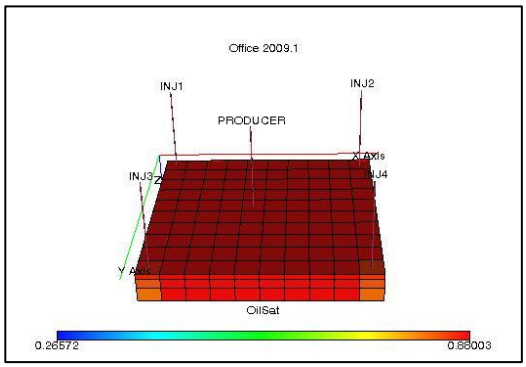


*Figure 38: 3D Historical Model on 28th November 1982*

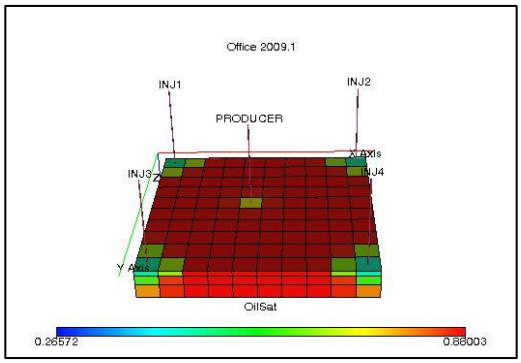


*Figure 41: 3D Historical Model on 11th February 1983*

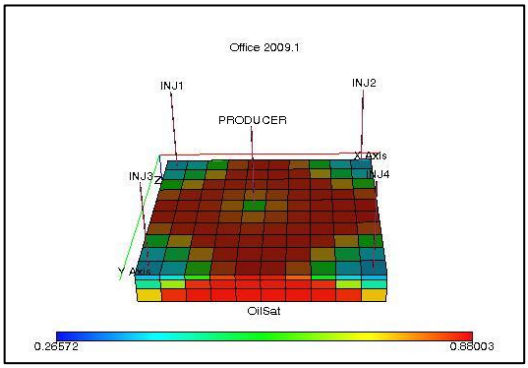


*Figure 40: 3D Historical Model on 6th June 1983*

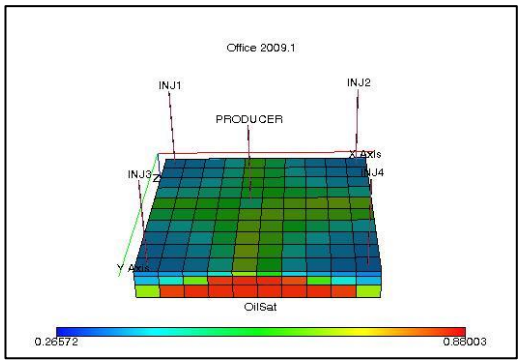


*Figure 39: 3D Historical Model on 27th March 1984*

### 6.2.2 Simulated Model

The simulated model is also built based on ODEH synthetic model but with different set of permeability. The permeability of historical model is multiplied by 1.5 to get a new set of permeability data for the simulated model. By having higher permeability compared to historical model, the sensitivity analysis is been analyzed to prove that changes in permeability can affect the production rate. Same as historical model, figures 42-45 are the 3 dimensional (3D) of simulated model at different time to demonstrate the changing of the color that represents oil and gas. Hence later, referring to the FOPT graph before, the gap between historical and simulated model will be reduced by applying two optimization methods to assisted history matching which are Kalman filter and steepest descent methods.

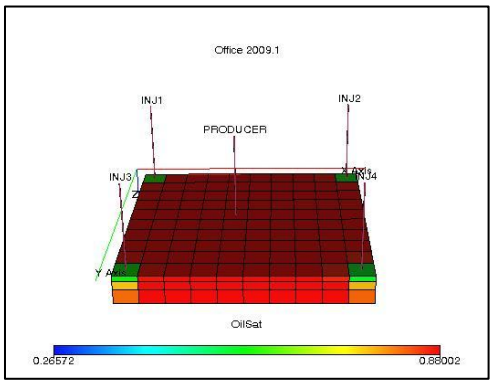


*Figure 45: 3D Simulated Model on 23rd December 1982*

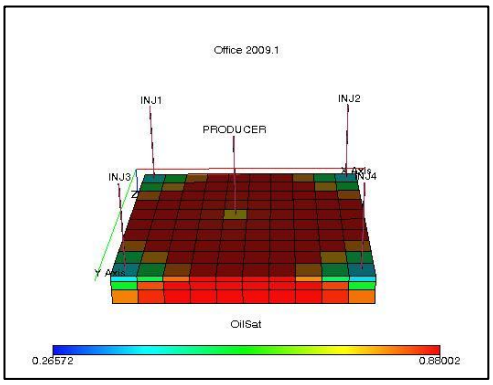


*Figure 44 : 3D Simulated Model on 8th March 1983*

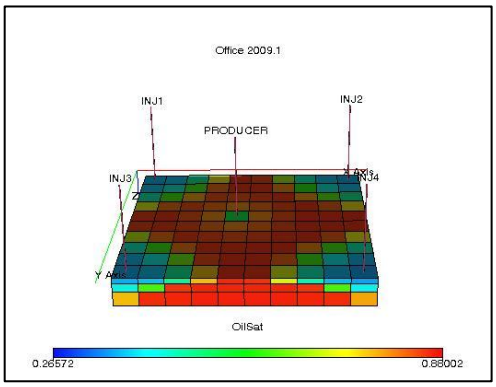


*Figure 43: 3D Simulated Model on 5th August 1983*

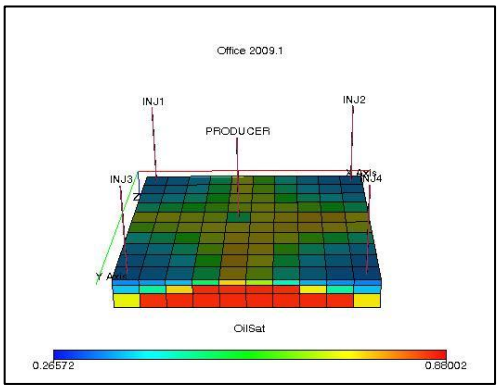


*Figure 42: 3D Simulated Model on 7th January 1984*

## 6.3 Comparative Analysis

Steepest descent path at each iteration is orthogonal to the previous direction. Hence the zigzags method in the design space is slightly ineffective. The algorithm will converge, but it may take an infinite iterations number. The convergence rate is linear. Regularly, a significant reduction is observed in the first few iterations, but after that the method will be very slow. It begins with a realistic convergence, but the progress will get slower as approaching the minimum. The technique may converge fast for bad scaled structures, but it depends on a good choice of initial point. In contrast, Kalman filter has a faster convergence as shown in the example. It also has presented less residual noise. To enable the convergence in less iteration, the important thing is to model the system more elegantly and estimate the noise more accurately.

In terms of root mean square error (RMSE), steepest descent has larger RMSE for all cases in the case study mentioned in literature review compared to BFGS and SSVM. On the other hand, Kalman filter has lower RMSE value than EnKF which leads to high accuracy and efficiency in permeability field estimation and the prediction after estimation.

In addition, Steepest Descent method can be applied when the minimum has been indicated, yet is commonly considered as a bad choice for any optimization problem. It is normally used only in combination with other optimizing techniques. However Kalman filter has been widely and successfully implemented for history matching purposes proved by many articles, thesis and journals. Table 8 simplifies the comparison between Kalman filter and steepest descent methods.

| Descriptions | Steepest Descent | Kalman Filter |
|---|---|---|
| Difficulty | Even though steepest descent is said to be simple, but it is difficult to compute the gradient for every iteration where it need a lot of derivations. | Kalman filter is easy to be implemented without the need of finding the gradient for each iteration since it is a non-gradient based method. |
| Convergence Time | The algorithm begins with a realistic convergence, but the progress getting slower as approaching the minimum. It may take an infinite iterations number. | Fast convergence. Convergence time can be improved by:<br>-Model the system elegantly<br>-Estimate the noise more accurately |
| Root Mean Square Error (RMSE) | Steepest descent has large RMSE for all waterflood cases compared to variable-metric minimization methods, BFGS and SSVM. | Kalman filter has lower RMSE value than EnKF which leads to high accuracy and efficiency in permeability field estimation and the prediction after estimation. |
| Applicability for History Matching | Steepest Descent method can be applied when the minimum has been indicated, yet is commonly considered as a bad choice for any optimization problem. It is normally used only in combination with other optimizing techniques. | Kalman filter is reliable and easy to be implemented. It has been widely and successfully implemented for history matching purposes such as updating facies location and parameters estimations of reservoir model |

**Table 8: Comparative Analysis of Steepest descent and Kalman filter**

# CHAPTER 7

# CONCLUSION AND RECOMMENDATION

## 7.1 Conclusion

A synthetic model is built to generate both historical and simulated model to apply two optimization methods which are Kalman filter and steepest descent techniques for history matching purposes. Kalman filter method is more efficient than other history matching methods in terms of computational burden and has recently provided promising results in terms of reservoir characterization and uncertainty quantification. From the literature review, it can be concluded that Kalman filter has been implemented more often and wider with higher accuracy, less uncertainties and faster convergence compared to steepest descent method.

## 7.2 Recommendation

In this project, one representative is going to be used from both gradient and non-gradient methods. This will pose a challenge for making conclusions regarding which is better. Interested individuals need to compare more methods in order to make a remarkable conclusion regarding the gradient and non-gradient methods. If deep study required, then more than one method will be compared. One method to be tested is not enough to conclude the whole history matching problem since history matching is a very wide system to be explored. Unfortunately, the study cannot go deeper within a very short period. Hence in future, it is fully recommended to continue this project into the next level by comparing more methods.

# REFERENCES


1. Heimhuber, R., *Efficient History Matching for Reduced Reservoir Models with PCE-based Bootstrap Filters*, 2012, University of Stuttgart: Sonthofen.
2. Tavassoli, Z., J.N. Carter, and P.R. King, *Errors in History Matching.* 2004.
3. Cardoso, M.A., *History Matching and Forecasting.* 2011.
4. Yang, P.H. and A.T. Watson, *Automatic History Matching With Variable-Metric Methods.* 1988.
5. Evensen, G., et al., *Using the EnKF for Assisted History Matching of a North Sea Reservoir Model*, 2007, Society of Petroleum Engineers.
6. Rwechungura, R.W., M. Dadashpour, and J. Kleppe, *Advanced History Matching Techniques Reviewed*, 2011, Society of Petroleum Engineers.
7. Jensen, J.P., *Ensemble Kalman Filtering for State and Parameter Estimation on a Reservoir Model*, 2007, Norwegian University of Science and Technology.
8. Bishop, G.W.G., *An Introduction to the Kalman Filter*, 2001, University of North Carolina at Chapel Hill.
9. G. Mahinthakumar, S.R.R., *Optimization-based Methodologies for Deteection and Monitoring of Groundwater Sources.* 2008.
10. McGill, *Numerical Optimization Algorithms*, (n.d).
11. Chen, D.S.O.Y., *Recent progress on reservoir history matching: a review.* 2010.
12. Van Doren, J., et al., *Adjoint-Based History Matching of Structural Models Using Production and Time-Lapse Seismic Data*, Society of Petroleum Engineers.
13. Dharmawan, M.A., et al., *New Approach To Validate History Matching Process*, 2013, Society of Petroleum Engineers.
14. Yang, C., et al., *Reservoir Model Uncertainty Quantification Through Computer-Assisted History Matching*, 2007, Society of Petroleum Engineers.
15. Dadashpour, M., *Reservoir Characterization Using Production Data and Time-Lapse Seismic Data*, 2009, Norwegian University of Science and Technology.

16. Zhang, D., H. Li, and H. Chang, *History Matching for Non-Gaussian Random Fields Using the Probabilistic Collocation based Kalman Filter*, 2011, Society of Petroleum Engineers.
17. Wang, X., *Method of Steepest Descent and its Applications*, 2008: University of Tennessee,.
18. Watson, A.T. and W.J. Lee, *A New Algorithm for Automatic History Matching Production Data*, 1986, Society of Petroleum Engineers.
19. Soonhong Cheong*, C.S., Sukjoon Pyun,Dong-Joo Min,Sangyong Suh, *Efficient calculation of steepest descent direction for source-independent waveform inversion using normalized wavefield by convolution*, 2004.
20. Taegong Seo and Changsoo Shin, D.-J.M., Sangyong Suh, *Efficient calculation of steepest descent direction of source signature independent waveform inversion of logarithmic wavefield*, 2004: Denver, Colorado.
21. Faragher, R., *Understanding the Basis of the Kalman Filter Via a Simple and Intuitive Derivation.* 2012.
22. Bishop, G.W.a.G., *An Introduction to the Kalman Filter.* 1997.
23. Maybeck, P.S., *Stochastic models, estimation, and control.* 1979.
24. Oliver D.S., R.A.C., Liu N, *Inverse theory for petroleum reservoir characterization and history matching*. 2008, United States of America by Cambridge University Press, New York.
25. Aanonsen, S.I., et al., *The Ensemble Kalman Filter in Reservoir Engineering--a Review.* 2009.
26. Kelly, A., *A 3D State Space Formulation of a Navigation Kalman Filter for Autonomous Vehicles*, 2006, Carnegie Mellon University.